AZIDE SUBSTITUTED PORPHYRINS WITH CROSSLINKING APPLICATIONS

FOR USE IN PHOTODYNAMIC THERAPY

By

DAVID FENWICK

B.Sc. (Hons), McGill University, 1998

A THESIS SUBMITTED IN PARTIAL FULFILLMENT OF

THE REQUIRMENTS FOR THE DEGREE OF

MASTER OF SCIENCE

In

The Faculty of Graduate Studies

(Department of Chemistry)

We accept this thesis as conforming

to the required standard

THE UNIVERSITY OF BRITISH COLUMBIA

February 2002

In presenting this thesis in partial fulfilment of the requirements for an advanced degree at the University of British Columbia, I agree that the Library shall make it freely available for reference and study. I further agree that permission for extensive copying of this thesis for scholarly purposes may be granted by the head of my department or by his or her representatives. It is understood that copying or publication of this thesis for financial gain shall not be allowed without my written permission.

Department of _Chemistry_

The University of British Columbia
Vancouver, Canada

Date _Feb 11 / 2002_

DE-6 (2/88)

Abstract

The objective of this work was to synthetically modify porphyrins such that they would possess a photoactive functionality which would chemically crosslink upon photoactivation for use in photodynamic therapy.

Three novel azide-modified porphyrins (**77, 86** and **101**) were synthesised, isolated and characterised. These were investigated for their ability to extrude N_2 on thermal and/or photochemical activation. Upon activation of **77**, the aldehyde (**39**) was formed.
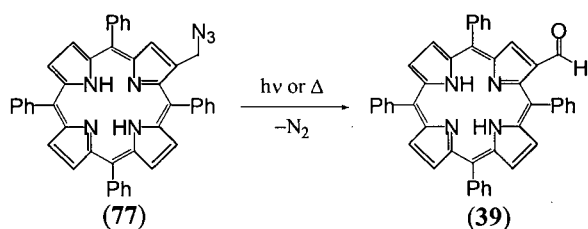
Activation of **86** led to a complex mixture where no pure compounds could be isolated or characterised.
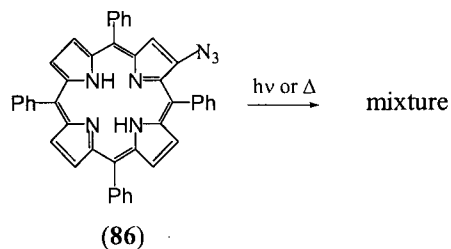
Activation of **101** gave a triplet derived product (**103**) in toluene, and a singlet derived

product (**104**) when activated in mesitylene.
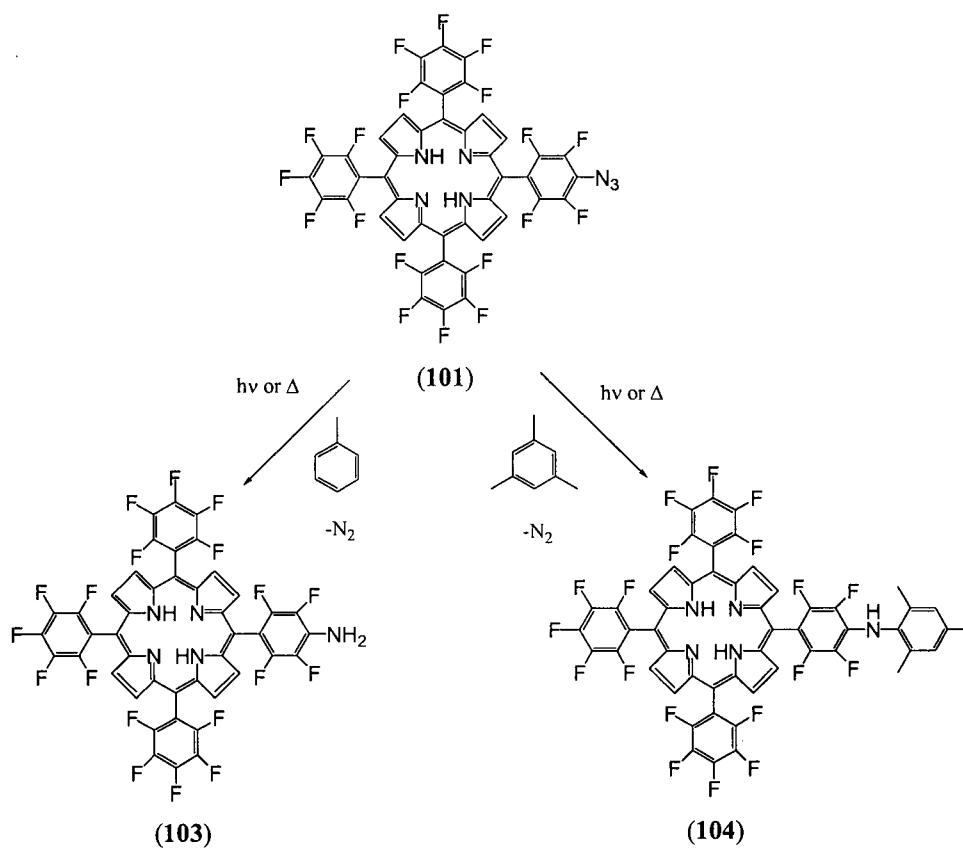
The synthesis toward *meso*-azido porphyrins as well as diazirine-modified porphyrins

were also carried out during the course of this work.

Table of Contents

1   Introduction

1.1   Tetrapyrrolic Macrocycles

List of Figures

List of Schemes

List of Tables

List of Abbreviations

ALA	5-Aminolaevulinic acid
ArN_3	Azido aryl compound
ArN_2^+	Diazonium aryl compound
ArI	Iodo aryl compound
$AgNO_2$	Silver nitrite
BPP	Bifunctional photoaffinity probe
CuOEP	2,3,7,8,12,13,17,18-Octaethylporphyrinatocopper(II)
CuTPP	5,10,15,20-Tetraphenylporphyrinatocopper(II)
CoTPP	5,10,15,20-Tetraphenylporphyrinatocobalt(II)
$Co(OAc)_2$	Cobaltous(II)acetate
CT	Charge transfer
DPP	5,15-Diphenylporphyin
DMF	N,N-Dimethylformamide
HOMO	Highest occupied molecular orbital
HpD	Hematoporphyrin derivative
ISC	Inter-system crossing
LUMO	Lowest un-occupied molecular orbital
MS	Mass Spectrometry
NaOAc	Sodium acetate
$NH_2OH \cdot HCl$	Hydroxylamine hydrochloride
NMR	Nuclear magnetic resonance
OEP	2,3,7,8,12,13,17,18-Octaethylporphyrin

POCl$_3$	Phosphorus oxychloride
PDT	Photodynamic therapy
pFTPP	5,10,15,20-Tetrakis(perfluorophenyl)porphyrin
PFPA	Perfluorophenyl azide
PP-DME	Protoporphyrin dimethyl ester
TFA	Trifluoroacetic acid
TPP	5,10,15,20-Tetraphenylporphyrin
TMS-CF$_3$	Trimethylsilyl trifluoromethane
TBAF	Tetrabutylammonium fluoride
TPAP	Tetrapropylammonium peruthenate
TLC	Thin layer chromatography
Zn(OAC)$_2$	Zinc acetate
ZnTPP	5,10,15,20-Tetraphenylporphyrinatozinc(II)

Acknowledgements

I would like to thank Professor David Dolphin for the opportunity to work in such a unique research environment. Many members of the Dolphin group have contributed to my learning experience over the past two and half years and I am grateful for all they had to offer. Ethan Sternberg, Elizabeth Cheu and Jeffery Flemming were all invaluable.

To Jamie Hepburn, Karen Macmillan, Shawn Walker, Arturo Orellana, Jeff MacArthur and Nariki Chun for making life in Vancouver worthwhile. Time was well wasted with all of you.

Finally to my family and friends back in Montreal who have always been there for me.

1   Introduction

1.1   Tetrapyrrolic Macrocycles

1.1.1   Background

Macrocycles consisting of four pyrrole units joined via methine bridges represent biological pigments that are responsible for much of the colour that is observed in nature. These pigments contribute to colours such as the green in grass as well as the crimson hue of blood. Representative tetrapyrrolic macrocycles are shown in Figure 1.1.

Porphyrin (1)

Chlorin (2)

Bacteriochlorin (3)

Isobacteriochlorin (4)
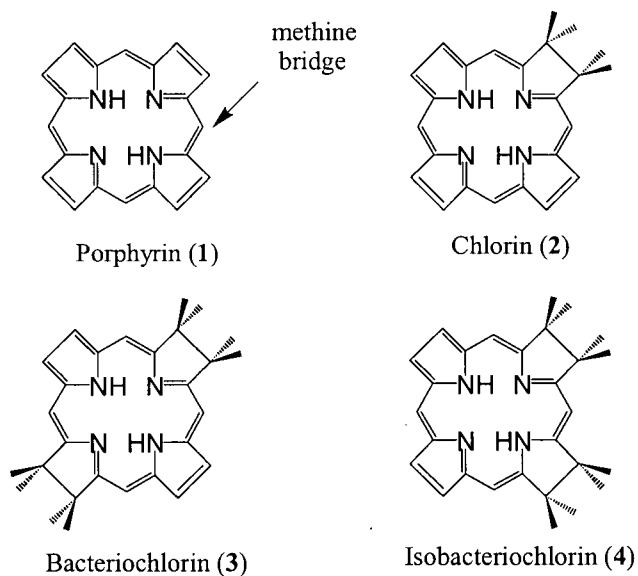
Figure 1.1. Tetrapyrrolic macrocycles.

The simplest porphyrin, porphine (1) is a fully unsaturated tetrapyrrolic macrocycle. A chlorin (2) is a porphyrin that has one reduced pyrrolic double bond. Bacteriochlorins (3) and isobacteriochlorins (4) are porphyrins that have two reduced double bonds on the antipodal and adjacent pyrroles, respectively.[1]

Porphyrins and porphyrin-like molecules share as similar purpose in nature, to bind metal atoms, which act as centres for important biochemical events such as photosynthesis and oxygen binding.[1] Two of the most important porphyrin-like molecules found in nature are chlorophyll-a (5) and heme (6) (Figure 1.2).

Chlorophyll-a

(5)

Heme

(6)

Figure 1.2. Structures of chlorophyll-a (5) and heme (6).

Magnesium, the central metal ion in chlorophylls, modulates the light absorbing and electron-transfer characteristics of the pigment and also serves as a binding centre for water.[1] This complex is the source of electrons for photosynthesis, a process that converts carbon dioxide to oxygen.[2] The function of these chlorophyll pigments (molecular antennae and reaction centre, Figure 1.3) is to capture photons in the near-red and red regions of the visible spectrum and convert this light energy into chemical energy via a series of electron transfer processes.[2]

Iron is the central metal ion found in heme. Hemoglobin and myoglobin are molecules that reversibly bind oxygen thus allowing either the transport or storage of oxygen,

respectively.[1] Hemoproteins are also involved in gene regulation, iron metabolism, drug metabolism and hormone synthesis.[1]
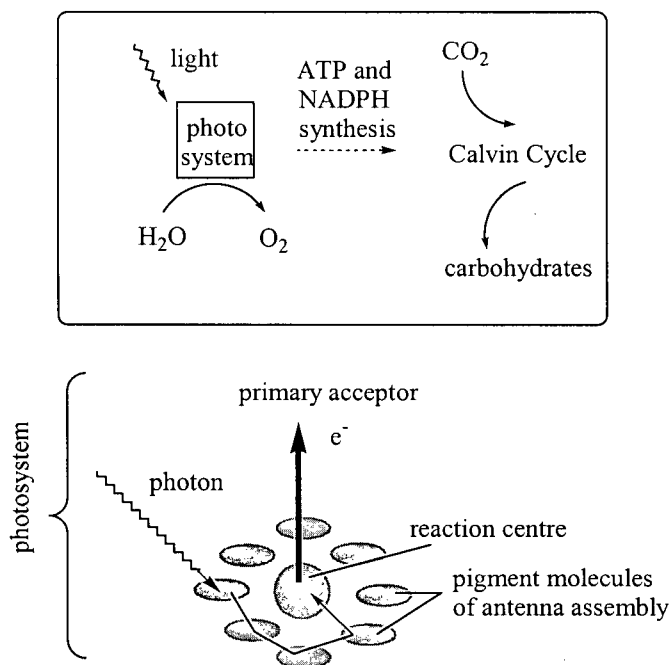
Figure 1.3. Simplified photosynthetic processes.

1.1.2 Nomenclature

Porphyrin nomenclature is based on the simplest fully unsaturated tetrapyrrolic macrocycle (Figure 1.4). Positions 2, 3, 7, 8, 12, 13, 17 and 18 are referred to as the β-positions; positions 5, 10, 15, 20 as the *meso*-positions; positions 1, 4, 6, 9, 11, 14, 16 and 19 are the α-positions. All substituted porphyrins can be named systematically with this system, however for convenience, naturally occurring porphyrins are named according to the trivial Fischer[3] nomenclature (Table 1.1).
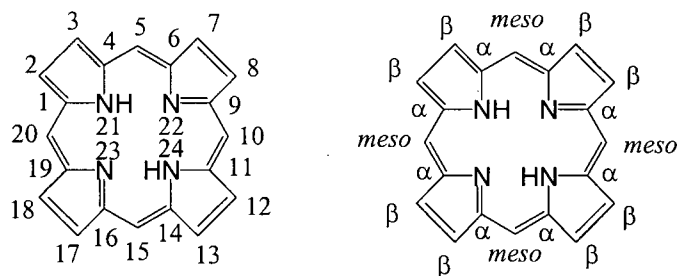
Figure 1.4. Porphyrin numbering and nomenclature.

Table 1.1.   Fischer nomenclature for selected naturally occurring porphyrins.

Trivial Name	Location[a] and Substituent[b]							
	2	3	7	8	12	13	17	18
Deuteroporphyrin	Me	H	Me	H	Me	PrH	Me	PrH
Hematoporphyrin	Me	Et(OH)	Me	Et(OH)	Me	PrH	Me	PrH
Mesoporphyrin	Me	Et	Me	Et	Me	PrH	Me	PrH
Protoporphyrin IX[c]	Me	Vn	Me	Vn	Me	PrH	Me	PrH
Uroporphyrin	AcH	PrH	AcH	PrH	AcH	PrH	AcH	PrH

[a] see numbering scheme (Figure 1.4). [b] Et(OH) = -CH(OH)CH$_3$, Vn = -CHCH$_2$, AcH = -CH$_2$COOH, PrH = -CH$_2$CH$_2$COOH. [c] roman numerals refer to Fischer's nomenclature for naming all the possible regioisomers of one set of substituents.

Two synthetic porphyrins, tetraphenylporphyrin (**7**) and octaethylporphyrin (**8**) are abbreviated TPP and OEP, respectively (Figure 1.5). Central metal complexes of these compounds are abbreviated ZnTPP or CuOEP for example.

TPP

(**7**)

OEP

(**8**)
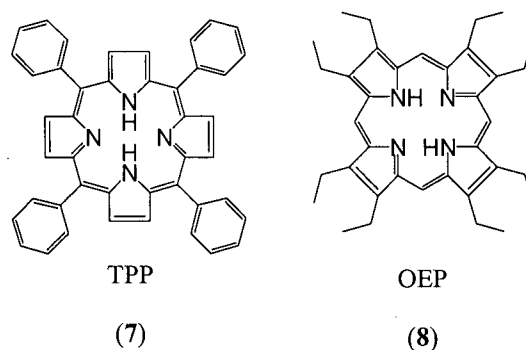
Figure 1.5. Tetraphenylporphyrin (TPP) and Octaethylporphyrin (OEP).

1.1.3 Synthesis of Porphyrins

Porphyrins are classified into two main groups, namely β-substituted porphyrins (such as OEP) and *meso*-substituted porphyrins (TPP for example). The β-substituted porphyrins resemble naturally occurring porphyrins while the *meso*-substituted porphyrins have no biological counterparts.[4]

1.1.3.1 Synthesis of β-Substituted Porphyrins

Naturally occurring porphyrins are synthesised from 5-aminolaevulinic acid (ALA) (**13**) (Scheme 1.1).[1] ALA is synthesised enzymatically from succinyl-CoA (**9**) and glycine (**10**) or from 2-oxoglutarate (**11**) and glutamate (**12**). ALA self-condenses with the help of ALA dehydrase to form porphobilinogen (PGB) (**14**), which condenses enzymatically with four other PGB molecules to give hydroxymethylbilane (**15**) which cyclizes to form uroporphyrinogen III (uro'gen III) (**16**). Uro'gen (III) is a key intermediate in the synthesis of many naturally occurring tetrapyrrolic macrocycles such as heme and chlorophyll (Figure 1.2).[1]

Symmetrical β-substituted synthetic porphyrins can be synthesised via condensation of monopyrrolic molecules.[5] Common methodologies include cyclization of 3,4-diethylpyrrole (**17**) with formaldehyde, followed by oxidation, to afford OEP in variable yields (55-75 %)[6] as well as reduction of 2-ethoxycarbonyl-3, 4-diethylpyrrole (**18**)

followed by acid catalysed tetramerization and subsequent oxidation of the
porphyrinogen (**20**) (Scheme 1.2.).[7]
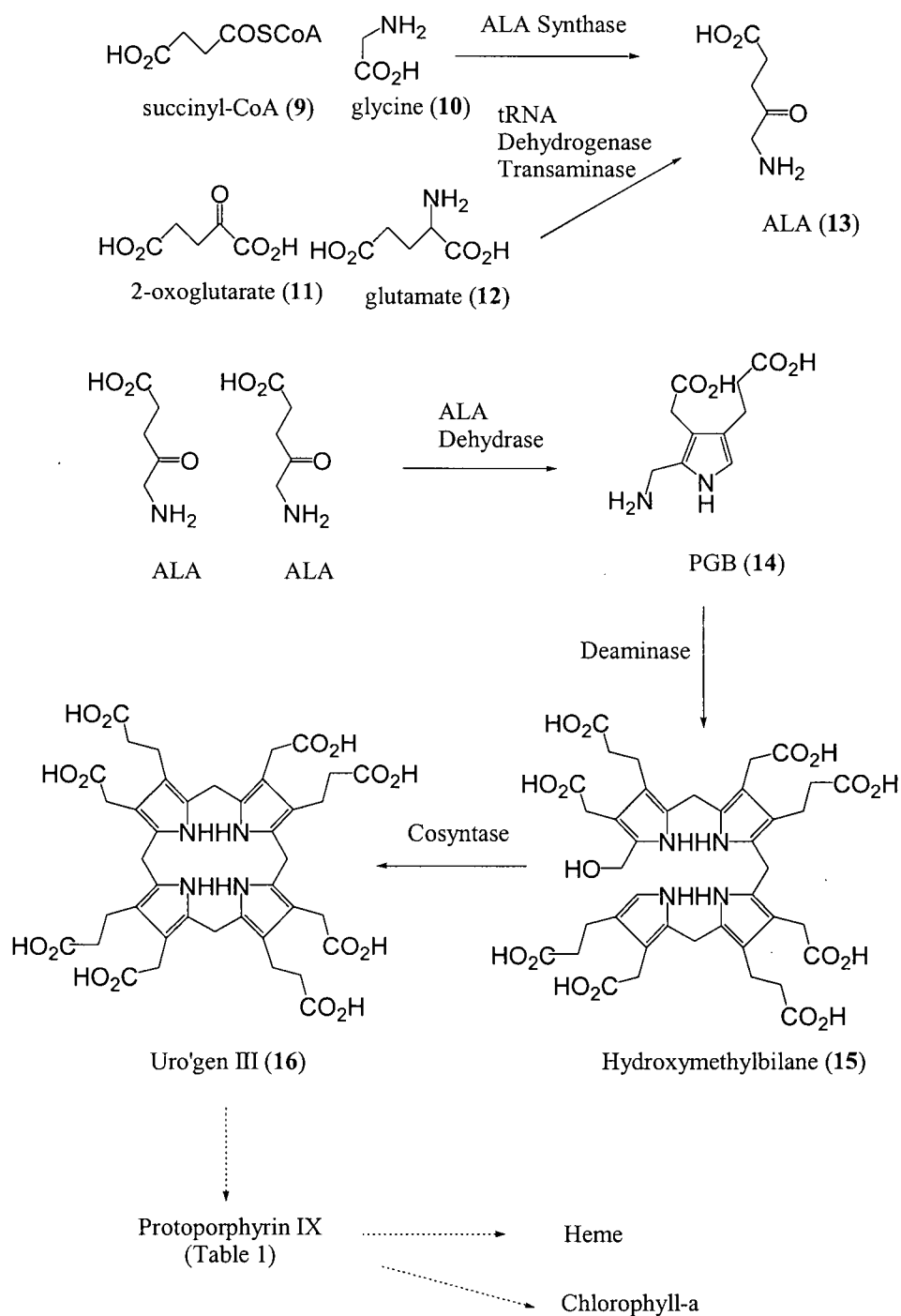
Scheme 1.1. Synthesis of Uro'gen III.
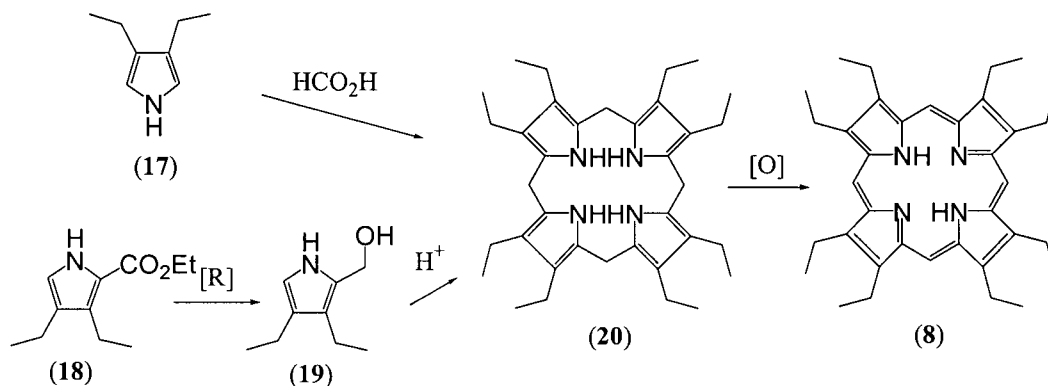
Scheme 1.2. Synthesis of OEP.

Unsymmetrical β-substituted porphyrins can be synthesised from dipyrrolic precursors.[5] Fischer's approach involved condensation of α-methyl dipyrromethenes **(21)** with α-bromo dipyrromethenes **(22)** in organic acid melts at high temperature (>200 °C) (Scheme 1.3).[8] The problem with using dipyrromethenes as dipyrrolic precursors for the synthesis of porphyrins is the harsh conditions needed to achieve coupling.

The Macdonald approach to synthetic porphyrins involves condensation of α-formyl dipyrromethanes **(23)** with α-unsubstituted dipyrromethanes **(24)** (Scheme 1.3).[9] This milder approach is favoured over that of Fischer due to the fact that dipyrromethanes with complex substituents are more readily prepared from pyrroles than the corresponding dipyrromethene analogues.[5]

(21) R₂ ... R₃ R₄ ... R₅ =NHHN— +

(22) R₂' ... Br + Br ... R₅' —NHHN= R₃' R₄'

(23) R₂ ... R₃ R₄ ... R₅ —NHHN— OHC CHO

(24) R₂' ... —NHHN— ... R₅' R₃' R₄'

Fischer Synthesis
Organic Acid melt
(>200°C)

MacDonald Synthesis
Acid Catalyst

R₂ ... R₃ R₄ ... R₅ —NH N=
R₂' ... N HN— ... R₅' R₃' R₄'
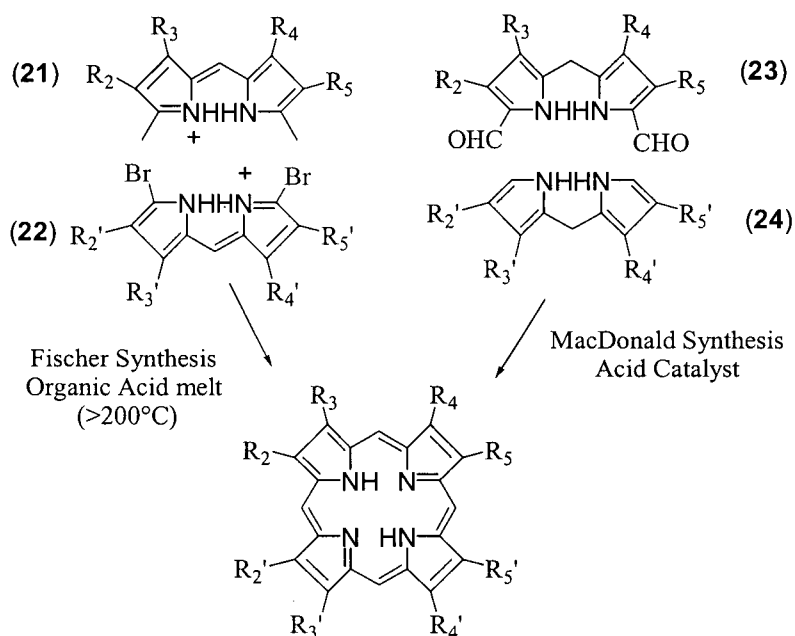
Scheme 1.3. Synthesis of unsymmetrical β-substituted porphyrins.

1.1.3.2 Synthesis of *meso*-Substituted Porphyrins

Rothemond first investigated the synthesis of *meso*-substituted porphyrins in 1935.[10] His methodology involved the condensation of an aldehyde (acetaldehyde or proprionaldehyde for example) with pyrrole in a sealed vessel at high temperatures (140-220 °C). In 1941 he described the synthesis of TPP.[11] Heating mixtures of benzaldehyde and pyrrole with pyridine in a sealed vessel at 220 °C for 48 hr gave TPP in 7-9 % yield. The notable features of Rothemond's syntheses are that the reactions are performed at high temperature and concentration (3-5 M of each reactant) in the absence of an oxidant.

Rothemond's approach left much to be desired.[12] The harsh conditions and low yields prompted Alder and Longo to investigate alternate syntheses of TPP in 1967.[12] They

performed condensations of benzaldehyde and pyrrole in organic acids in vessels open to the atmosphere (air being the oxidant). The use of acetic acid resulted in TPP being obtained in 30-40 % yield. The use of proprionic acid (reflux, 141°C) reduced the yield (20 %) but the product was reported to crystallise faster, facilitating the isolation of purer TPP.

The Alder method allowed for efficient syntheses of a variety of *meso*-substituted porphyrins, notably tetra-aryl porphyrins with diverse aryl substituents on multi-gram scales.[13] However, the harsh reaction conditions preclude the use of benzaldehydes bearing sensitive functional groups (esters and dioxanes, for example).[13] The large amount of tar produced presents purification problems, especially with porphyrins that do not crystallise at the end of the reaction.[13] Batch-to-batch reproducibility is also reported to be a problem.[13] Lindsey more recently investigated the synthesis of tetraphenylporphyrins in order to overcome the shortcomings of, and compliment the Alder method.[13]

Lindsey focused on the synthesis of tetraphenylporphyrins under equilibrium conditions.[13] He reported that pyrrole and the desired aldehyde react reversibly at room temperature with acid catalysis to form a cyclic tetraphenylporphyrinogen (**27**, Scheme 1.4) at thermodynamic equilibrium.[13] The porphyrin (**29**) is subsequently obtained (35-50 %) after oxidation of the porphyrinogen (**27**) with DDQ (**28**).

Due to the peculiarity of porphyrin chemistry, (difficulty with purification, low solubilities, susceptibility to oxidation and reduction, photosensitivity, etc.) it is desirable to perform as many synthetic transformations as possible prior to forming the porphyrin.[13] The mild conditions of the Lindsey method allow for the use of many pre-functionalized aldehydes, which were not suitable using the Alder method.
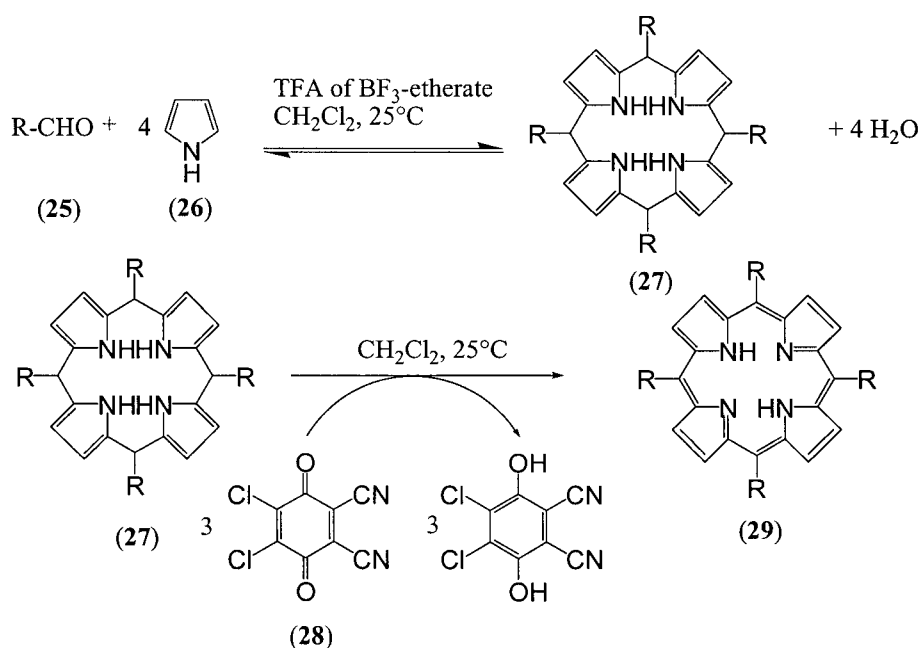
Scheme 1.4. Synthesis of TPP (Lindsey method).

1.1.4 Structural Characteristics and Reactivity

Kuster in 1912 first suggested that the structure of a porphyrin consisted of a tetrapyrrolic macrocycle, although it was universally thought that such a large ring would be intrinsically unstable.[14] However, in 1929, Fischer completed the total synthesis of heme, thus the tetrapyrrolic macrocycle that Kuster suggested became accepted.[15]

Porphyrins are aromatic molecules that contain a total of 22-conjugated π-electrons, 18 of which are incorporated into the delocalized pathway. The remaining four reside in the π-orbitals of the inner nitrogen atoms (Figure 1.6). The porphyrin system is in accord with Huckel's [4n+2] rule for aromaticity.[16] One or two cross-conjugated double bonds of a porphyrin may be reduced without substantial loss of the macrocyclic aromaticity.[17] Reduction of one double bond leads to the formation of a chlorin, while reduction of two yields a bacteriochlorin (Figure 1.1).
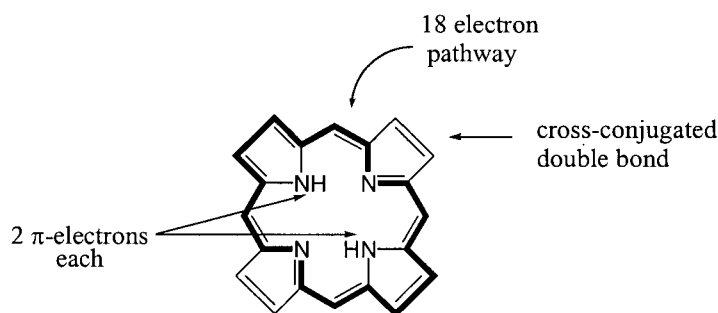
Figure 1.6. Aromatic pathway of a porphyrin.

As a result of this aromaticity, porphyrins have a large ring current. This ring current is best observed using ^{1}H-NMR spectroscopy. Significant shielding and deshielding effects brought on by this diamagnetic ring current can shift inner pyrrole protons as far upfield as –5 ppm, and the *meso* and β-protons as far downfield as 10 ppm.[18] It is important to note that the inner pyrrole protons are localized equally on all four nitrogen atoms. This is due to the fact that porphyrins exist equally as 2 tautomers (Figure 1.7). The inner nitrogen atoms can be protonated to give the corresponding monocation (pK_3 = 5) and dication (pK_4 = 2). They can also be de-protonated to produce the porphyrin dianions ($pK_1 \approx pK_2 \approx 16$).[19]
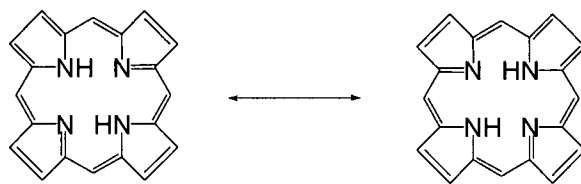
Figure 1.7. Tautomeric forms of a porphyrin.

Porphyrins can form complexes with a wide array of metals that can adopt a number of different oxidation and co-ordination states.[20] The central metal ions in metalloporphyrins have an important inductive effect on the macrocyclic π-system and significantly alter reactivity at the porphyrin periphery. Metals such as Mg(II), Zn(II) and Cd(II) (d^0 and d^{10} metals) are incapable of dπ-pπ back-bonding.[17] These metals induce the highest electronegativity at the porphyrin periphery and are very labile under mildly acidic conditions. Metals such as Fe(II), Co(II), Cu(II) or Ni(II) (d^6-d^9) can accept electron density from the porphyrin to their partially filled d-orbitals via π-backbonding.[17] This decreases the electron density at the porphyrin periphery and partially inhibits peripheral reactivity. Metals with d^1-d^5 configurations contain empty d-orbitals and are highly electrophilic. These metals tend to favour reactivity at the β-position.[17]

Woodward first proposed generalisations on the reactivity of porphyrins based on valence bond considerations in 1962.[21] He proposed that the two pyrrole units could be considered to have their own aromatic sextet of π-electrons while each pyrrolene unit is one electron short of an aromatic sextet. These pyrrolenes withdraw electron density from the neighbouring *meso*-carbons in order to compensate for this deficiency. These

generalisations predicted greater electrophilic character for the *meso*-positions relative to the β-positions.

Theoretical *ab initio* self-consistent field-molecular orbital (SCF-MO) calculations predict that reactivity (namely, electrophilic, nucleophilic and radical reactions) at the porphyrin periphery should take place preferentially at the *meso*-position.[22]

The aforementioned generalisations predict that the *meso*-positions are electronically more reactive than the β-positions. However, when nearby β-positions are substituted, the *meso*-positions are sterically less accessible. In these cases, the β-positions are favoured to undergo substitution or addition reactions.[17] Hence, both steric and electronic effects play roles in peripheral reactivity.

1.1.5 Functionalization of Porphyrins

Most functionalization studies are related to TPP and resemble electrophilic aromatic substitution. Peripheral functionalization was not investigated until 1968 when the first electrophilic bromination was reported.[23]

Porphyrin functionalization can be compared to those of three model systems: benzene, pyridine and alkenes.[24] Benzene chemistry is typified by electrophilic aromatic substitution. Porphyrins also undergo electrophilic substitutions and can be regarded as 18-π-electron analogues of benzene. In electrophilic substitution, metallation of the

porphyrin is necessary in order to protect the inner nitrogen atoms from the deactivating effect of protonation.[24] Reactions at the inner nitrogen lone pairs, including protonation, alkylation[25] and N-oxide formation[26] are similar to those of pyridine. Porphyrins undergo chemical reactions that parallel those of simple alkenes via partial isolation of the peripheral double bonds.[27] This partial isolation can be achieved via nitration, which will be discussed in Section 1.1.5.2.

Much of the research presented in this thesis involves substitution at the porphyrin periphery followed by modifications to the functional group. The chemistry of formylation and nitration is of particular interest as these two functional groups lend the substituted porphyrin open to a wide array of modifications.

1.1.5.1 Formylation of Porphyrins

β-Formylation of TPP using the Vilsmeier reagent (DMF and POCl$_3$) creates a versatile intermediate for further modification.[24] Core metallation with Ni(II), Cu(II) or Co(II) is necessary as metals such as Mg(II) and Zn(II) do not withstand acidic conditions.[24] The mechanism of β-formylation is shown in Scheme 1.5. Attack on the iminium salt (31) followed by loss of HCl yields (32), which is readily hydrolysed under basic conditions to give the desired aldehyde (33).
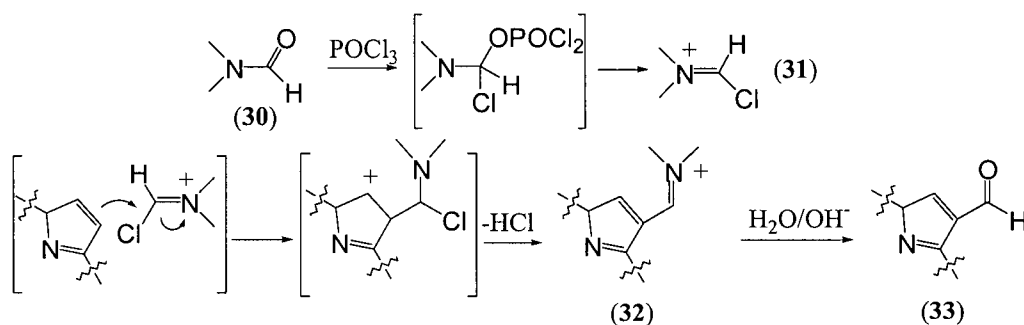
Scheme 1.5. β-Formylation with Vilsmeier reagent.

β-Formylation of CuTPP with excess Vilsmeier regent in chloroform followed by hydrolysis was reported to give β-formyl-CuTPP (**34**) in 95 % yield.[28] Treatment of β-formyl-CuTPP with H_2SO_4 (conc.) did not demetallate the porphyrin, but rather catalysed an intramolecular cyclization to yield ketone (**35**) (Scheme 1.6).[29]
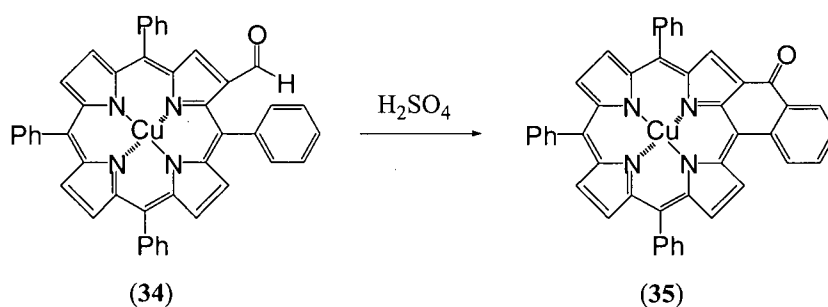
Scheme 1.6. Treatment of β-formyl-CuTPP with H_2SO_4.

β-Formyl-TPP can be obtained in moderate yield (13-50 %) using the Fe(III) complex, Fe(TPP)Cl.[30] The reaction of choice, as Reported by Ponomarev and co-workers, involves CoTPP (**36**) and the Vilsmeier reagent in 1,2-dichloroethane followed by demetallation with H_2SO_4 before hydrolysis of the intermediate iminium salt (**38**)

(Scheme 1.7).[31] This procedure gives the desired free base formylated porphyrin (**39**) in upwards of 65 % yield after chromatographic work up. Formyl-OEP (*meso*-substituted) is obtained similarly using CuOEP. [32]
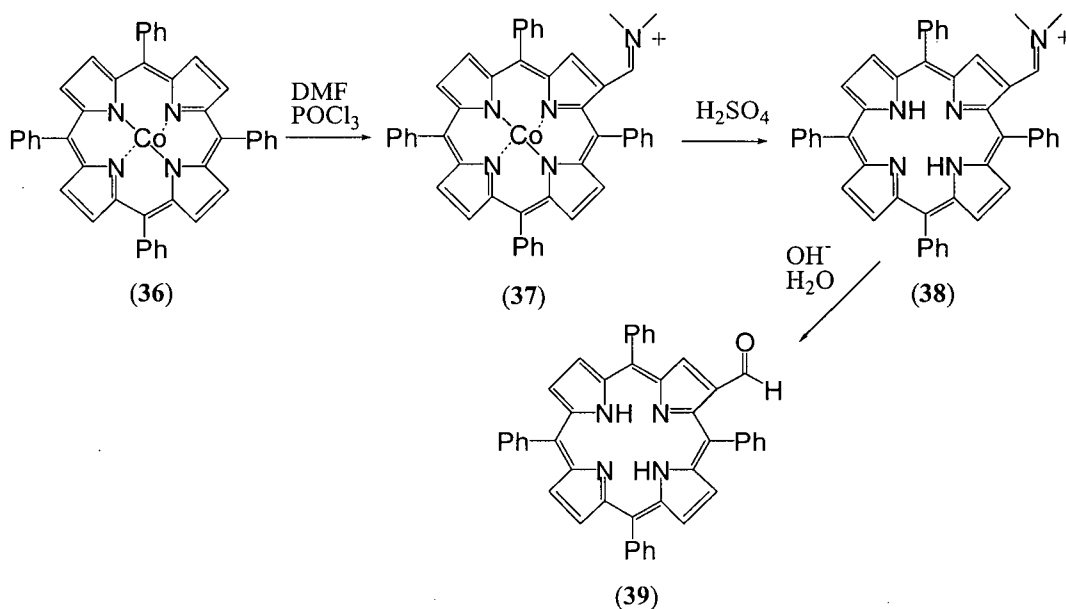
Scheme 1.7. Formylation of CoTPP.

The formyl group can be synthetically modified in a number of ways. Conversions to the corresponding oxime,[33] acrylate,[34] vinyl[35] and ylide[36] porphyrins, as well as numerous other modifications have been reported. A comprehensive review of all these conversions would give further insight into the versatility of this functional group, but is beyond the scope of this work.

1.1.5.2 Nitration of Porphyrins

Porphyrins can be nitrated via electrophilic aromatic substitution using fuming HNO_3 and acetic acid[37] as well as with mixtures of HNO_3 and H_2SO_4.[38] Nitration can also be

achieved via oxidation of the porphyrin with I_2 to give the porphyrin π-cation radical (40) followed by treatment with $AgNO_2$.[39] Nucleophilic addition to the porphyrin is thought to be followed by the removal of an electron and a proton (Scheme 1.8).[40]

$$P\text{-}H + 1/2\ I_2 \longrightarrow [P\text{-}H]^{\bullet +} + I^- \xrightarrow{AgNO_2} [H\text{-}P\text{-}NO_2]^{\bullet} + AgI \xrightarrow[-H^+]{1/2\ I_2} P\text{-}NO_2 + HI$$

$$\qquad\qquad\qquad\qquad (40)\qquad\qquad\qquad\qquad\quad (41)\qquad\qquad\qquad\qquad\qquad (42)$$
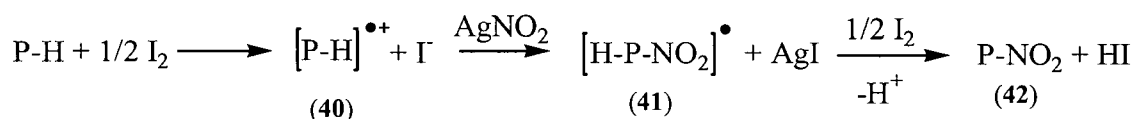
Scheme 1.8. Nitration of Porphyrins.

The nature of the attacking species (NO_2^- or $NO_2^{\bullet}$) has been the subject of debate. Barnett and Smith proposed that the attacking species was NO_2^-.[41] Johnson and Dolphin suggested the oxidation of NO_2^- to $NO_2^{\bullet}$ by excess I_2 followed by attack on the porphyrin π-cation radical.[42]

Porphyrins that contain a nitro group in the β-position possess unique reactivities that facilitate peripheral functionalization.[24] β-Nitroporphyrins are subject to classic nitro aromatic chemistry such as reduction, diazotization and subsequent nucleophilic displacement.[43] β-Nitroporphyrins also behave similarly to nitroalkenes in that they undergo nucleophilic addition with various nucleophiles.[44,45] They also facilitate electrophilic substitution on the antipodal pyrrole ring (Figure 1.8).[46]
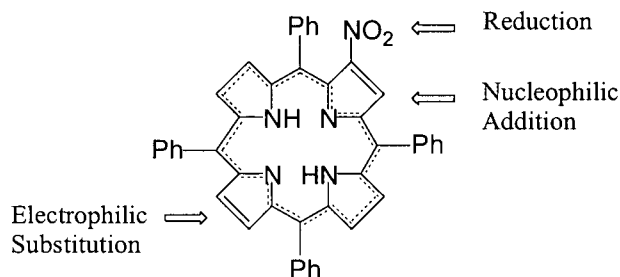
Figure 1.8. Reactivity of β-nitro-TPP.

1.1.6 Optical Absorption Spectra

Porphyrins absorb light energy at a variety of wavelengths. There are two main regions in the UV-visible spectrum where porphyrins absorb, the more intense absorption band, between 390 and 425 nm, is called the Soret band.[1] The origin of this band is a result of the second excited state and has molar extinction generally from 2 to 4 x 10^5 $M^{-1}cm^{-1}$.[1] Free-base porphyrins (metal free) exhibit four weaker Q bands in the UV-visible spectrum, which are labeled in increasing order of wavelength IV, III, II and I. These originate from the first excited state and vibrational modes and have molar extinction coefficients on the order of 10^{-4} $M^{-1}cm^{-1}$.[1] Porphyrins are classified according to their Q band intensities. There are four such classes, namely *etio*, *rhodo*, *oxo-rhodo* and *phyllo*-type (Figure 1.9). If the β-substituents are alkyl groups and the relative intensities are such that IV > III > II > I, the spectrum is classified as an *etio*-type spectrum. *Rhodo*-type spectra are observed when electron-withdrawing groups are at the β-positions. As a result, these intensities are such that III > IV > II > I. *Oxo-rhodo*-type spectra (III > II > IV > I) are observed if electron-withdrawing groups are on opposite pyrrole units. When

the β-positions are un-substituted or *meso*-positions filled, a *phyllo*-type spectrum is observed (IV > II > III > I).[47]
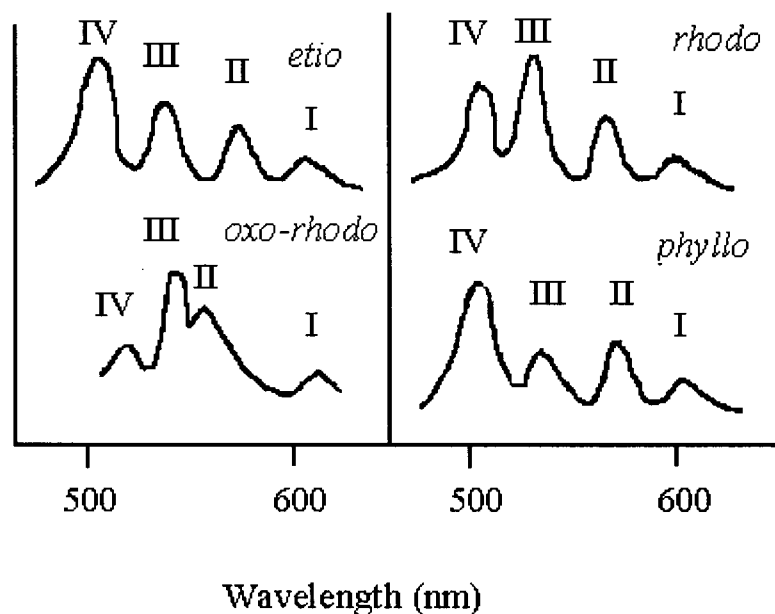
Figure 1.9. UV-visible spectra of porphyrins showing Q bands I-IV.

Free-base porphyrin spectra are markedly different from metalloporphyrins (Figure 1.10). This difference arises from the fact that the inner pyrrolic hydrogen atoms reduce the conjugated ring symmetry from D_{4h} (metalloporphyrin) to D_{2h} (free-base porphyrin).[48] The increase in symmetry upon incorporation of a metal into the core of a porphyrin results in collapse of four Q-bands into two or one.[48] A similar spectral simplification is observed upon formation of the porphyrin dication by addition of a strong acid.
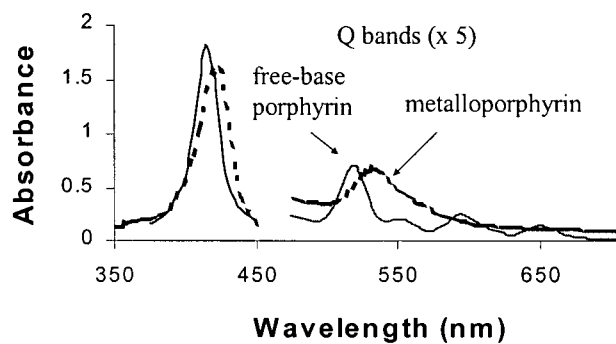
Figure 1.10. UV-visible spectra of free-base (solid line) and metallo- (dashed line) porphyrins.

A marked increase in intensity of the highest wavelength Q band, as well as a red shift characterises chlorins (solid line) and bacteriochlorins (dashed line) (Figure 1.11).
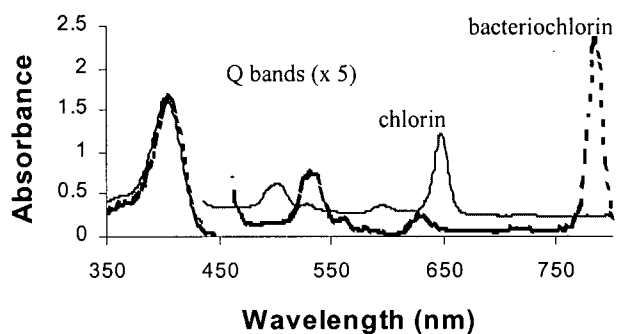
Figure 1.11. UV-visible spectra of a chlorin (solid line) and bacteriochlorin dashed line).

Gouterman examined the physical basis for these observations.[48, 49]   Figure 1.12 presents

a scheme based on theoretical calculations for the four generic metalloporphyrin* classes.

The longest wavelength absorption in porphyrins and chlorins can be assigned as a

HOMO-LUMO transition ($\pi \rightarrow \pi^*$). The energy of the HOMOs (a_{u1}) are progressively

raised with increasing saturation, while the LUMOs in porphyrins, chlorins and

bacteriochlorins remain relatively isoenergetic (the LUMO energy in isobacteriochlorins

are raised). The larger the HOMO-LUMO gap, the higher energy needed for the

transition. A lower energy transition represents longer wavelength absorption.
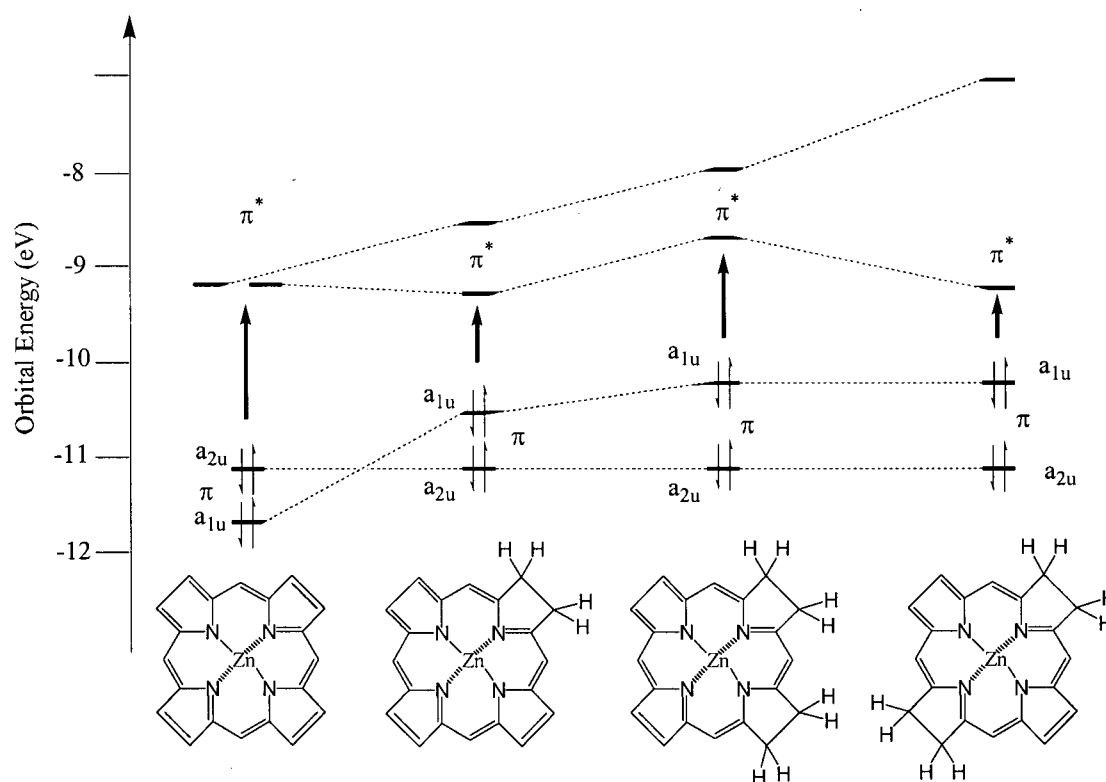
Figure 1.12. Energy level diagram for the frontier orbitals of the four generic
metalloporphyrin classes (adapted from Fajer[50]).

---

* Metalloporphyrins and chlorins are shown for simplicity. The same trend is observed in the analogous
free-base macrocycles.

1.1.7   Porphyrins as Photosensitizers

A molecule in an excited state may transfer its excess energy to another molecule in a process called photosensitization.[51] This process allows the creation of excited states that otherwise would not be produced from direct irradiation. For example, energy transfer from the excited triplet state of a donor molecule, $D^{*(\uparrow\uparrow)}$, to an acceptor molecule in its electronic ground state, $A^{(\uparrow\downarrow)}$, produces the ground state of the donor and the triplet exited state of the acceptor (Scheme 1.9).

$$D^{*(\uparrow\uparrow)} + A^{(\uparrow\downarrow)} \rightarrow A^{*(\uparrow\uparrow)} + D^{(\uparrow\downarrow)}$$
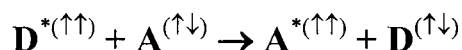
Scheme 1.9. Photosensitization of an acceptor (A) by a donor (D).

Porphyrins are photosensitizers and the mechanism of photosensitization is best illustrated in a Jablonski diagram (Figure 1.13). The photosensitizer absorbs light energy promoting an electron from the ground singlet state (S_o) to an excited singlet state (S_1). The first excited singlet state can decay to the ground state radiatively via fluorescence, or non-radiatively via internal conversion. The molecule can undergo the spin-forbidden process of inter-system crossing (ISC) resulting in the excited triplet state. The excited triplet state can decay radiatively via phosphorescence or undergo two ˙kinds of reactions.[52] This triplet state can participate in an electron-transfer process with a biological molecule to form radicals and radical ions which upon interaction with O_2 can produce the superoxide ion, O_2^- (Type I reaction).[52] This triplet state can also undergo a

Type II reaction which results in the conversion of molecular triplet oxygen ($^3O_2$) to the highly reactive singlet oxygen ($^1O_2$) (an energy transfer reaction).[53]

· Photodynamic therapy (PDT) is a medical treatment that capitalises on the ability of photosensitizers to produce reactive intermediates such as singlet oxygen to treat a variety of diseases.

Type I Reaction
(Free radical process)

S_1 4

O_2

2   3 T_1

O_2^- (superoxide)

$^1O_2$

6

1   5

Type II Reaction

$^3O_2$

S_o

1. Absorption; 2. Nonradiative Decay;
3. Fluorescence; 4. Intersystem Crossing;
5. Phosphorescence; 6. Energy Transfer
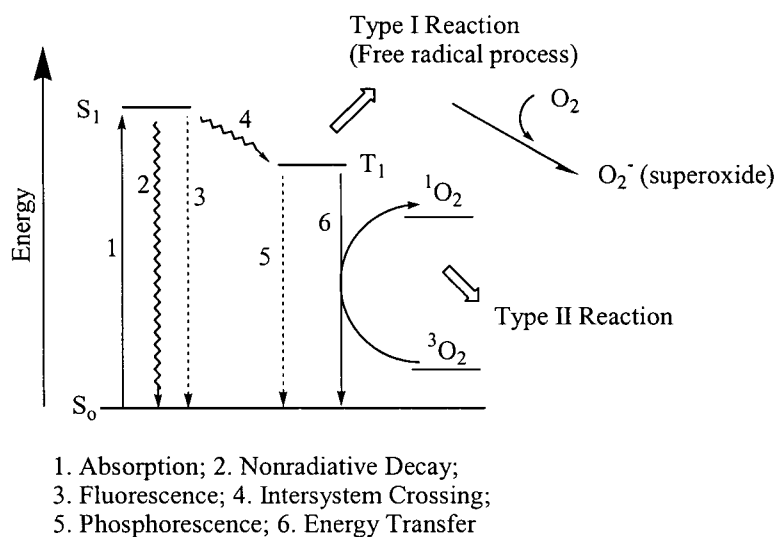
Figure 1.13. Modified Jablonski diagram of a photosensitizer.

1.2   Photodynamic Therapy

1.2.1   History

In 1913, Meyer-Betz injected himself with 200 mg of hematoporphyrin (Hp) (Table 1.1, p. 4) and suffered no ill effects until he exposed himself to sunlight, whereupon he suffered swelling and remained photosensitive for several months.[54] Auler and Banzer

reported that Hp had an affinity for cancerous tissue.[55] The localisation of Hp into cancerous tissue was qualitatively assessed by fluorescence measurements.[56] Schwartz and co-workers proposed that the selective fluorescence of cancerous tissues after administration of Hp was due to an impurity rather than Hp itself.[57] This led Lipson and co-workers to develop a derivative of Hp that increased the amount of cancer-localising component in the drug.[58]

Hematoporphyrin derivative (HpD) was first prepared by reacting Hp with acetic acid/sulfuric acid (9:1) and then treating the intermediate mixture with aqueous sodium hydroxide.[58] Lipson reported that HpD was taken up and retained in tumours to a greater extent than pure Hp.[59] In 1978, Dougherty reported on a series of patients showing a positive response in tumours treated with HpD and light.[60] Purified HpD is known as Photofrin® and has been approved in several countries for various cancer treatments.

1.2.2   Mechanism of Cell Necrosis

Photodynamic therapy (PDT), a medical treatment, utilises a photosensitizer and light of a certain wavelength to elicit a cytotoxic effect on diseased tissue such as tumours or abnormal blood vessels.[61] The cytotoxic agent in PDT is assumed to be singlet oxygen ($^1O_2$) (Section 1.1.7.).[62] $^1O_2$ is a powerful, fairly indiscriminant oxidant that reacts with a variety of biological molecules, such as amino acids (tryptophan, **43**) and steroids (cholesterol, **44**) giving the corresponding endoperoxide and hydroperoxide, respectively (Scheme 1.10.).[62]

The lifetime of $^1O_2$ in cellular components ranges from 100 ns in lipids to 250 ns in the cytoplasm.[63] As such, the diffusion range of $^1O_2$ in cellular media is predicted to be approximately 45 nm.[64] The diameter of human cells range from 10 to 100 μm, hence $^1O_2$ cannot diffuse more than a single cell length.[65] Ideally the site where $^1O_2$ is generated is at the site of attack. The superoxide ion (O_2^-) may also be involved in some aspects of PDT damage.[66] The mechanism of cellular necrosis is believed to be due to several factors including vascular shutdown,[67] direct cell killing[68] and apoptosis.[69]
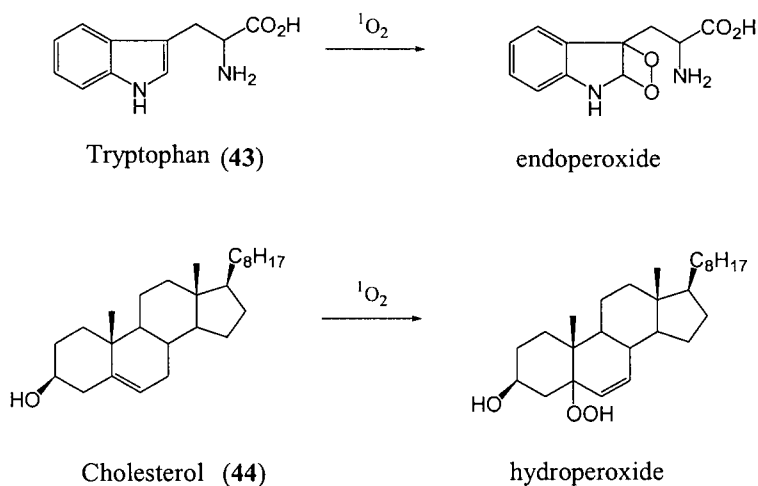
Scheme 1.10. Example of the reactions of singlet oxygen with biological molecules.

1.2.3   Requirements for a PDT Drug

Photosensitizers for use in PDT should have certain requirements.

- The candidate should be chemically pure. This simplifies dose-response relationships. With a multi-component drug (Photofrin®) the interpretation of the causes for the overall effect becomes difficult.[70]

- It should have significant absorption in the 650-800 nm region. The absorption and scattering of light increases as the wavelength decreases and the most efficient photosensitizers have strong absorption bands in the long wavelength region.[71] Light penetration in tissue drops off significantly below 550 nm. It doubles from 550 nm to 630 nm and doubles again in going to 700 nm. This is followed by a 10 % increase upon going to 800 nm (Figure 1.14). However a shift beyond 800 nm is undesirable. First the photosensitizer becomes more susceptible to photo-bleaching.[72] Secondly, efficient energy transfer may not be possible. The wavelength of absorption refers to the excited singlet state, the triplet state is of lower energy. If the triplet level of the photosensitizer were below that of singlet oxygen (24.5 kcal/mol), transfer of energy would be difficult.
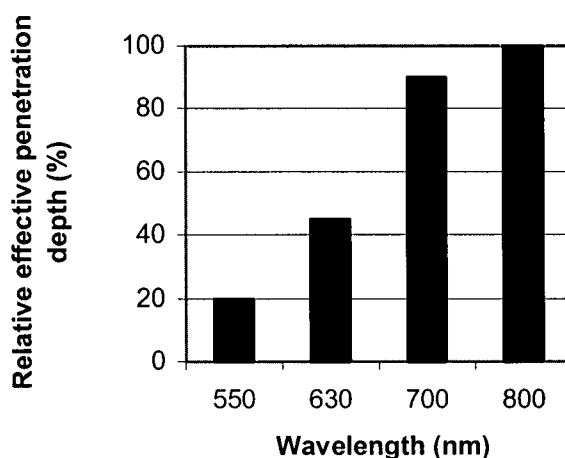
Figure 1.14. Wavelength penetration through human tissue.

- It should have a high quantum yield of singlet oxygen.[52] This is necessary to achieve efficient destruction of cells. Most photosensitizers currently under clinical trials for PDT are porphyrin-based molecules.[64]

- It should accumulate in tumours preferentially.[70] The mechanism of tumour localisation is not known, however as with HpD, porphyrins tend to accumulate preferentially in diseased tissue.

- It should display minimal dark toxicity.[52] The advantage of PDT drugs is that they can be introduced systemically and activated site-specifically, in order to minimise damage to surrounding healthy tissue. If the drug is active in the absence of light (dark toxicity), then this benefit is lost.

- Other desirable qualities include facile synthesis and simple formulation.[52]

The energy transfer capabilities of porphyrins make PDT possible. As mentioned in Section 1.1.7., porphyrins in their excited states can transfer their energy to acceptor molecules. Porphyrins can also physically lose an excited electron in electron transfer processes. These two phenomena are of particular interest as the research presented in this thesis (Ch. 2. Results and Discussion) involves electronic-interchromophore communication between porphyrins and photoactive functionalities.

1.3   Photoinduced Electron Transfer in Porphyrin Systems

In photosynthesis, carotenoids provide photoprotection by rapidly quenching chlorophyll triplet states that are formed in the antennae systems or photosynthetic reaction centres (Figure 1.3).[73] This triplet-triplet energy transfer prevents chlorophyll-sensitised production of singlet oxygen, which is damaging to the photosystem.[74] Carotenoids also function to quench the first excited singlet state of chlorophyll via energy transfer, electron transfer, or some other process leading to internal conversion. [75, 76]

Like photosensitization, electron transfer processes require donor-acceptor pairs. In donor-acceptor pairs whose separation and orientation are not constrained, electron transfer is diffusion controlled and occurs from the excited triplet state.[77] Diffusion controlled electron transfer is not possible from excited singlet state as they do not have long enough lifetimes.[77] In order for electron transfer to occur on a shorter time scale (from an excited singlet state) donor-acceptor separation must be constrained. This is achieved by incorporating a covalent bonding network.[77] Besides providing the necessary constraints, the bonding network may also provide a mechanism for orbital overlap so that the net donor-acceptor electronic interaction is increased.   In photosynthesis, for example, protein components hold the various donor and acceptor species at precise separations, allowing for efficient electron transfer through the complex network of chromophores. [77]

The majority of dyad models for photoinduced electron transfer consist of porphyrins covalently linked to quinones. Kong and Loach prepared the ester linked dyad (**45**, Figure 1.15) in 1978,[78] and the amide (**46**) was reported by Tabushi *et al.* in 1979.[79] It has been shown that these types of systems undergo photoinduced electron transfer as shown in Figure 1.16.
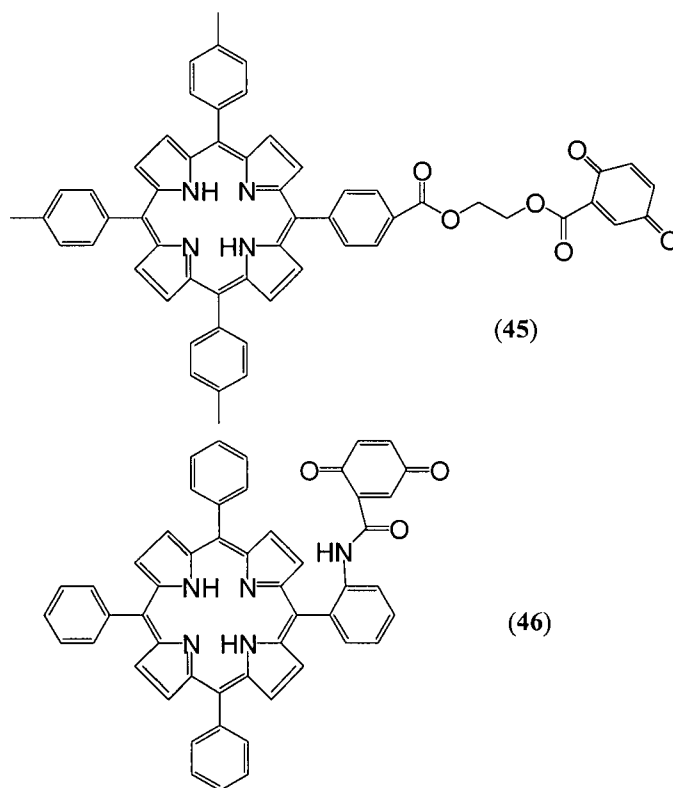
Figure 1.15. Representative porphyrin-quinone dyads.

Excitation of the porphyrin gives the first excited singlet state (^{1}P-Q). This state may decay by the usual pathways of internal conversion, fluorescence and intersystem crossing to the triplet state. Competing with these processes, is donation of an electron to the quinone to give a charge separated state (P^+-Q^-). This state has a certain fraction of

the energy of the excited singlet state. Eventually this state recombines to give the P-Q

ground state and release the stored energy as heat.[80]
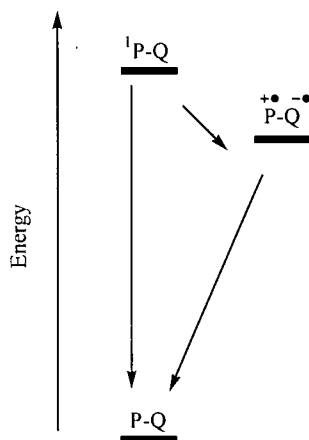
Figure 1.16. Interconversion pathways for a porphyrin-quinone dyad.

Other systems that mimic photosynthetic electron transfer include carotenoid-porphyrin-

quinone triads (Figure 1.17).[73] The interconversion pathway for such a triad consists of

similar states to those shown in Figure 1.16, namely (C-^{1}P-Q), (C-P$^+$-Q$^-$) and (C$^+$-P-Q$^-$)

where the carotenoid (C) acts as an electron donor.

(47)
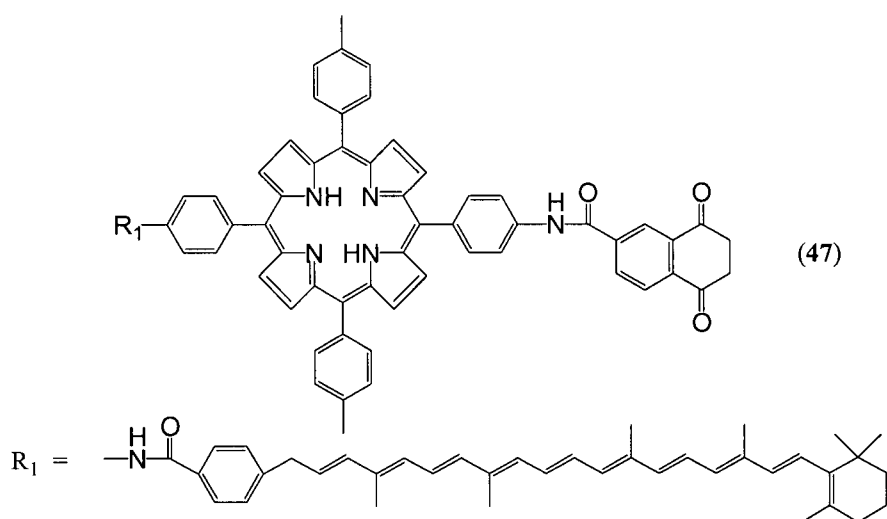
Figure 1.17. A carotenoid-porphyrin-quinone triad.

It is hoped that electronic communication between porphyrins and covalently bonded chromophores can be capitalised upon for use in photoaffinity labeling, which will be described in the next section.

1.4   Photoaffinity Labeling

In a typical photoaffinity labeling experiment the objective is to derivatize the site where a macromolecule (receptor) binds its natural ligand (Figure 1.18).[81] By this means it is possible to identify the component of a mixture that binds a particular ligand. The ligand is typically modified with a photoactive functionality and must be a close structural analogue of the natural ligand. [82]

Figure 1.18. Photoaffinity labeling of a receptor R by a photoaffinity reagent L.

Westheimer[83] and Knowles[84] are credited with introducing photochemical reagents for the formation of covalent bonds with macromolecules. Since their initial application, photochemical reagents been widely used in the chemical/biochemical community.[85] Aryl azides are the most often used class of photochemical reagents.[82]

There are certain requirements that must be taken into account when designing a photoaffinity reagent.

- The photochemical reagent must be stable in the dark and in the presence of constituents of a biological sample.[82]

- The reagent must absorb light at a suitable wavelength. Most reagents are designed to absorb above 300 nm as proteins and nucleic acids absorb strongly below 300 nm and therefore hinder activation of the photolabel.[86] However, for the objectives of the work presented in this thesis, the desired reagent will be a porphyrin derivative for use in PDT. As such, it is hoped that the porphyrin-modified reagent will be activated by red light ($\lambda = 650$ nm).

- The intermediate formed by photolysis should be short lived and highly reactive. This can be problematic as many aryl azides tend to undergo reaction with nucleophiles rather than undergo C-H insertion, even in the C-H rich hydrophobic core of membranes.[87]

- The adducts formed in the photolabeling reactions must be stable.[82]

- The last requirement is ease of synthesis. Aryl azides are commonly employed as their synthesis is achieved with relative ease.[88]

1.4.1 Aryl Azides

The photochemistry of aryl azides is summarized in Scheme 1.11.[82] Four reactive intermediates are thought to be involved: the singlet and triplet nitrene (**48**), fully bonded electrophiles (seven-membered cyclic ketenimines, **49**) and the anilinyl radical (**50**) which is generated when the triplet nitrene abstracts a hydrogen atom from a donor (RH). These species undergo reactions primarily with C-H bonds, nucleophiles (amines) and oxygen. Dimer (**51**) formation is also common.[89]
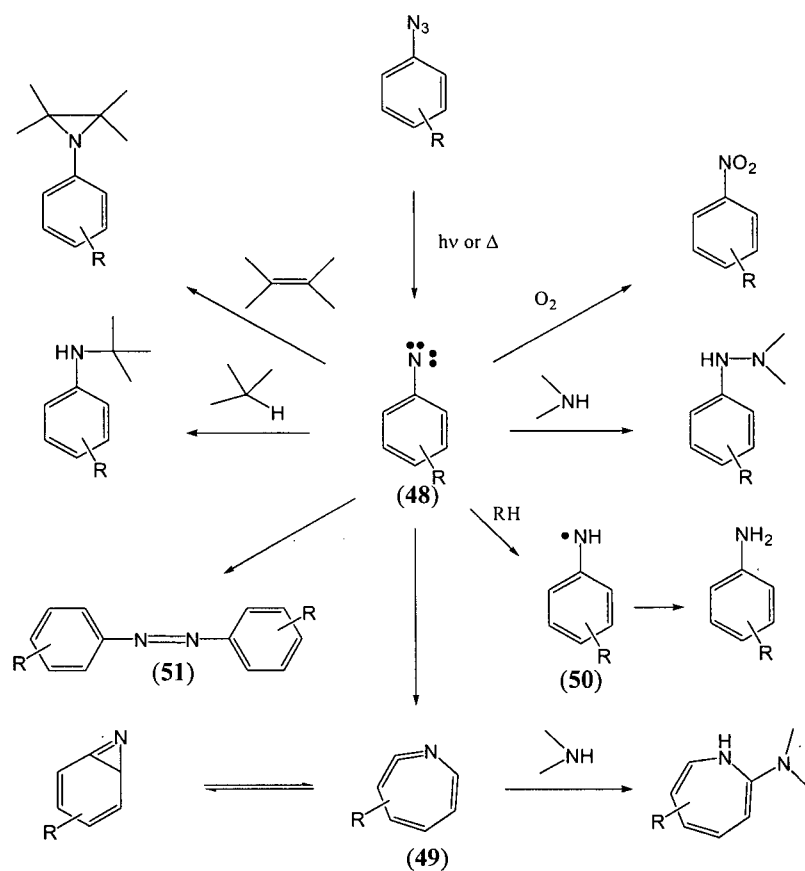
Scheme 1.11. Photochemistry of aryl azides.

Electron-withdrawing substituents on the aromatic ring have substantial effects on the reactivity of aryl azides. Notably, electron withdrawing groups are known to decrease the lifetimes of the triplet nitrene intermediate as well as making the intermediate more susceptible to nucleophilic attack, thereby decreasing the yield of C-H insertion.[90, 91]

The most general and widely used method to synthesise aryl azides is diazotization of the corresponding amine followed by addition of sodium azide (Scheme 1.12).[92] Aryl azides can also be obtained via nucleophilic displacement of nitro-substituted benzenes.[93]

$$Ar—NH_2 \xrightarrow{HNO_2} Ar—N_2{}^+ \xrightarrow{NaN_3} Ar—N_3$$
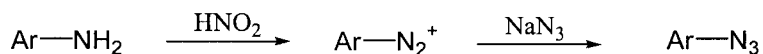
Scheme 1.12. Synthesis of aryl azides.

An aryl azide label was used recently by de Montellano *et al.* to identify hemoprotein active site residues and defined their location with respect to the heme iron atom.[94] Reaction of myoglobin with *meta*-(azidophenyl)diazene (**52**) gave the corresponding σ-bonded *meta*-phenyl-iron complex (**53**) (Scheme 1.13). Photolysis, followed by shift of the aryl group from the iron to the porphyrin nitrogens attached the heme chromophore to the labelled protein residue. Since aryl azides undergo ring expansion, there are two possible insertion mechanisms. The nature of the bond between the probe and the amino acid residue was not defined in this study, as the mass spectrometric fragmentation patterns are consistent with both cross-linking mechanisms. Digestion of the modified protein and mass spectrometric analysis of the peptides identifies His-64 as the residue to which the heme is attached.
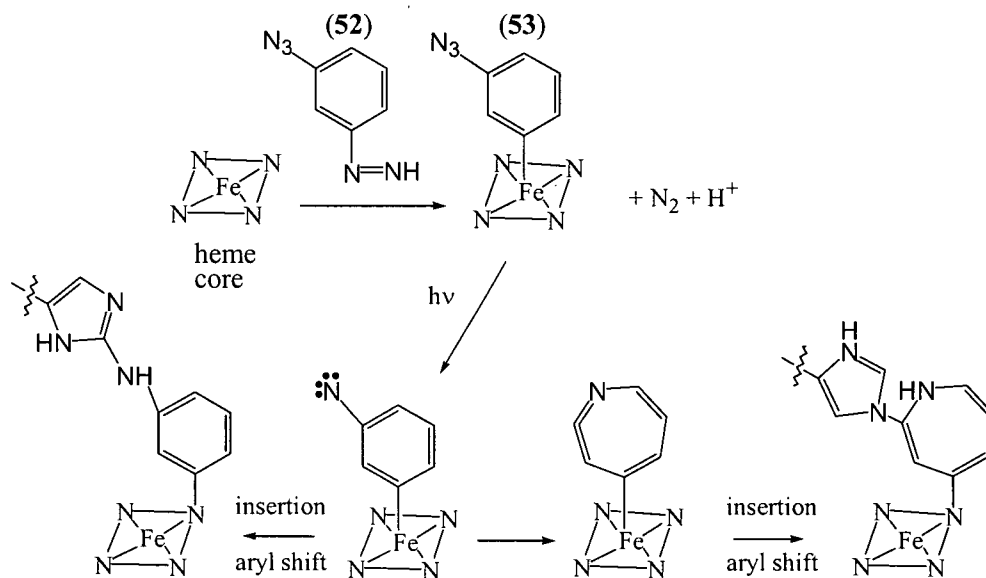
Scheme 1.13. Alkylation of protein component (His-64) by nitrene and keteneimine forms of the photolyzed *meta*-azidophenyl-iron probe.

1.4.2 Perfluorophenyl Azides

Even though aryl azides are among the most widely used reagents for photoaffinity labeling studies, photolysis of simple phenyl azides at room temperature in hydrocarbon solvents gives minimal amounts of intermolecular C-H insertion products.[95] The reactions are rarely clean, and polymeric tars often accompany minimal amounts of identifiable products.[96] Yields of azide photolabeling are generally less than 30 %.[97-101]

Banks reported that perfluorophenyl azide(s) (PFPA) showed promise as an improved series of photolabels.[102] It was shown that thermal decomposition of 4-azidotetrafluoropyridine (**54**) in cyclohexane gave 45 % yield of C-H insertion product.[102] Dunkin reported that pentafluorophenyl nitrene did not undergo ring expansion photochemically.[103] Platz reported that photolysis of pentafluorophenyl azide (**55**) at 25 °C gave high yield of C-H insertion into toluene[104] and in cyclohexane.[105] Scheme 1.14 depicts these reactions.
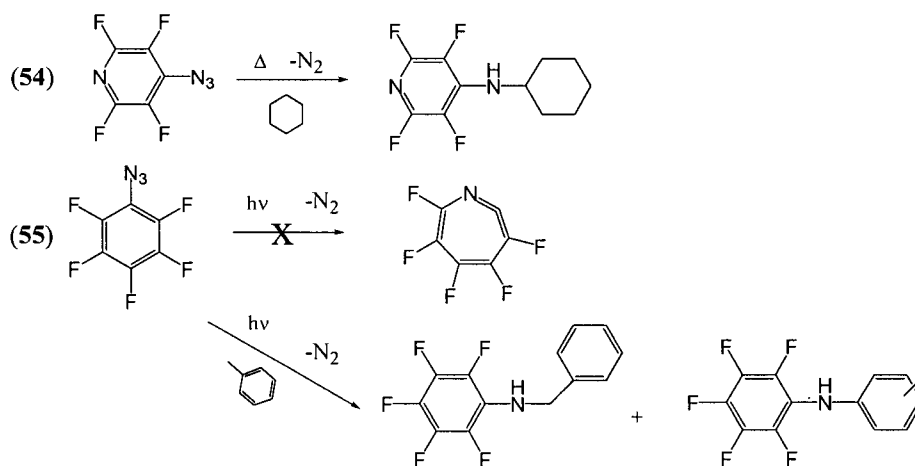
Scheme 1.14. Perfluorophenyl azide reactivity.

Scheme 1.15 depicts the reaction of a fluorinated aryl azide (**56**) with toluene as reported by Keana.[106] Photolysis of ArN_3 gives an excited species that can decompose to give the singlet nitrene or the triplet nitrene that can react with toluene. C-H insertion by singlet nitrenes is thought to be a one step process, as such singlet nitrenes should not differentiate between the methyl C-H or the C-H of the aromatic ring.[107] However with regard to triplet nitrenes, C-H insertion involves hydrogen abstraction followed by successive hydrogen abstraction or radical recombination. Therefore, since the ring C-H bond is stronger than the methyl C-H bond,[108] triplet nitrenes should show preference for

abstraction of a benzylic hydrogen over a ring hydrogen in toluene. Introduction of the electron withdrawing nitro-group was shown to promote the formation of triplet products, mainly the aniline.

$$ArN_3 \xrightarrow[-N_2]{h\nu} \left[ArN \right]^{*1} \xrightarrow{ISC} \left[ArN \right]^{*3}$$

Ar = (structure with F, F, F, X, CO$_2$Me)

(56) X = F, NO$_2$

X	CH$_2$NHAr	NHAr	NHAr	CH$_2$NHAr	ArNH$_2$
	a	b	c	a	d
			% Yield		
F	16	13	9	16	29
NO$_2$	8	\	\	8	71

Singlet products   Triplet products
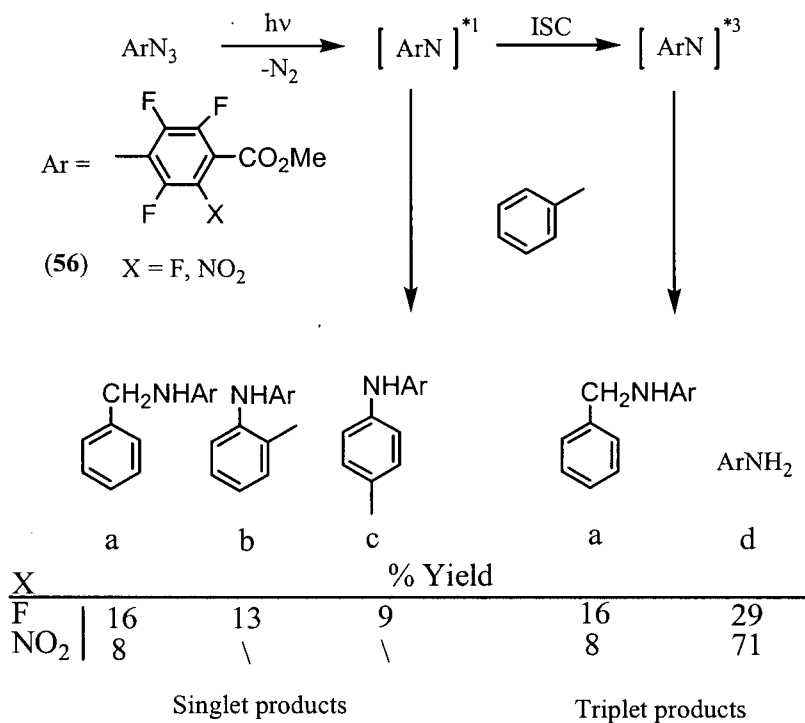
Scheme 1.15. Perfluorophenyl azide photochemistry.

It is known that pentafluorophenyl compounds containing electron-withdrawing groups, such as pentafluorobenzonitrile (57) react with sodium azide to give 1,4-disubstituted compounds (58) regioselectively (Scheme 1.16).[109] It is also known that 5,10,15,20-tetrakis-pentafluorophenylporphyrin (pFTPP) (59) undergoes fluorine substitution with a variety of nucleophiles, including lithium diethyl amide (Scheme 1.17).[110]
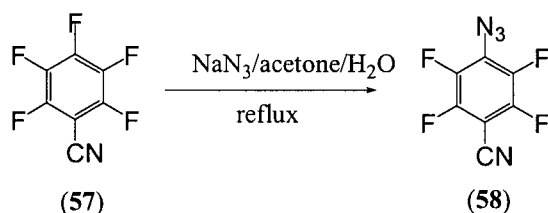
Scheme 1.16. Synthesis of perfluorophenyl azide derivative.
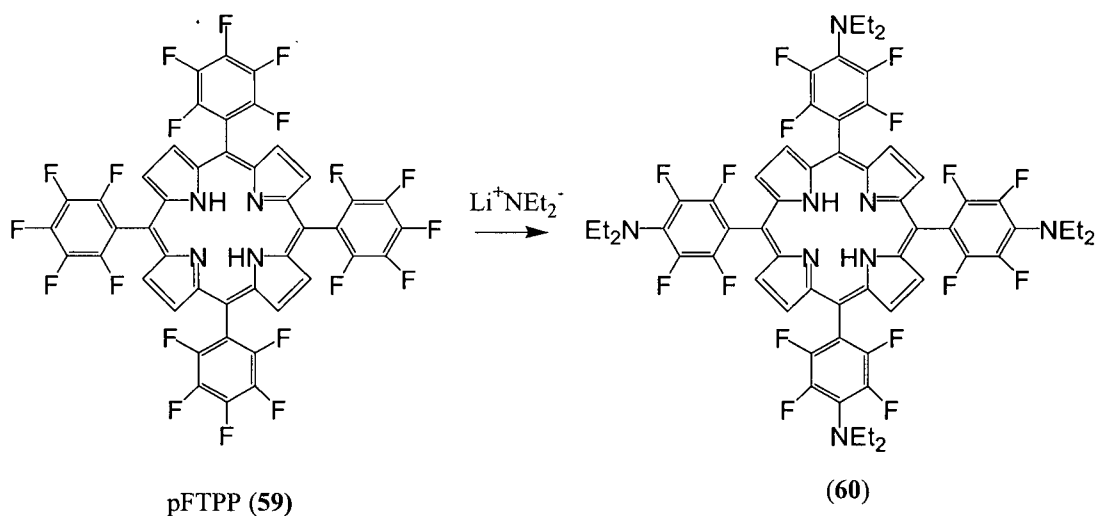
Scheme 1.17. Nucleophilic substitution of pFTPP.

It was thought that pFTPP would be able to undergo fluorine substitution with NaN_3 and an azide-derivatized fluorinated porphyrin was envisioned for the work presented in this thesis.

1.4.3 Diazirines

Smith and Knowles introduced diazirines as potential photochemical reagents in 1973.[111] Recently 3-trifluoromethyl-3-phenyldiazirines have been held in high regard as they satisfy many of the criteria for the ideal reagent listed on p. 32.[112]

Irradiation of a diazirine (61) has been shown to give both carbene (62) and a linear diazo species (63) (Scheme 1.18).[82] Carbenes can insert into C-H bonds to give species such as (64). These types of diazirines are, in many ways thought to be superior photoaffinity labeling reagents than simple aryl azides in that they are more reactive and have fewer photolysis by-products.[112]
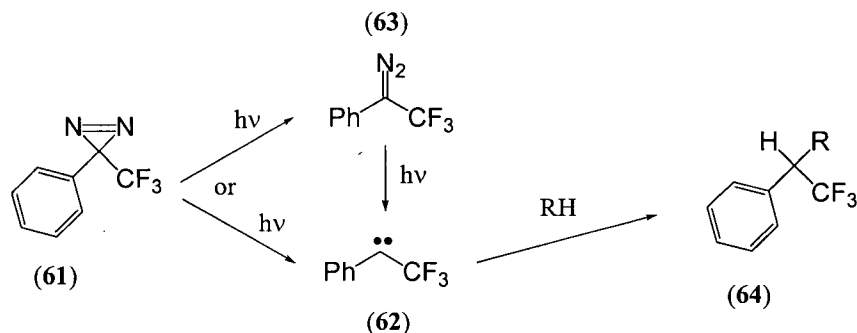
Scheme 1.18. Photochemistry of 3-trifluoromethyl-3-phenyldiazirines.

Trifluoromethyldiazirines are generally synthesised via the route shown in Scheme 1.19.[112] The trifluoroketone (65) is converted to the corresponding oxime (66) with $NH_2OH \cdot HCl$, which is protected with TsCl to give 67. Treatment with ammonia yields a diaziridine (68), which is oxidized to the corresponding diazirine (69).
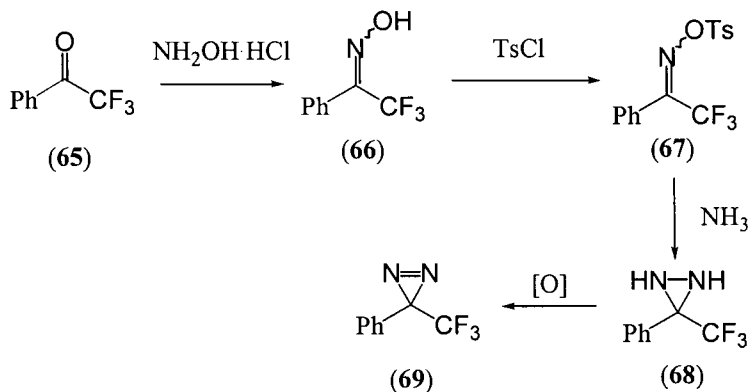
Scheme 1.19. Synthesis of trifluomethyldiazirine.

Ojima and co-workers reported on a novel bifunctional photoactive probe (BPP) (Figure 1.19) for the study of paclitaxel-microtubules interaction.[113] Paclitaxel (a taxoid) is an important chemotheraptic agent for the treatment of various cancers.[114] Clarifying the binding site of paclitaxel at microtubules serves to develop a rational basis for drug design.
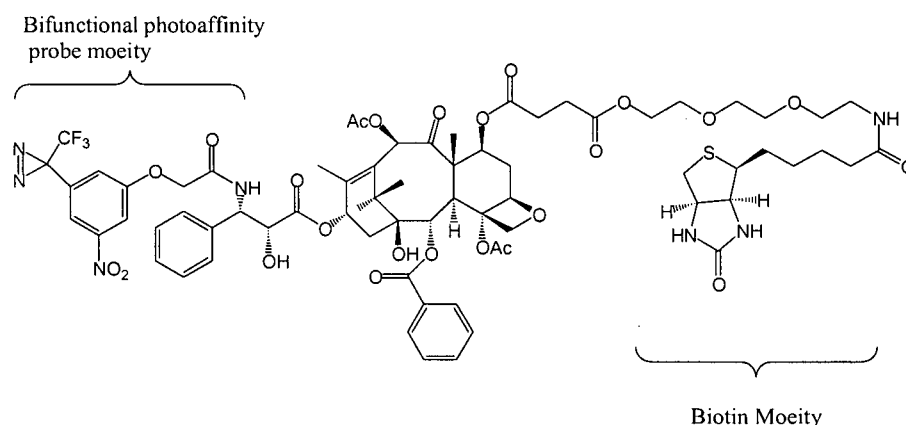
Figure 1.19. Taxoid photoaffinity labeling probe.

The photoaffinity labeling process envisioned in this case involves the following (Scheme 1.20): (i) the BPP-taxoid is bound to the microtubules (receptor) and photolyzed (site A); (ii) the receptor is cleaved; (iii) the crosslinked peptide fragments are separated from the non-fragmented fragments (the biotin tag facilitates separation); (iv) the taxoid is cleaved from the crosslinked peptides by site B photocleavage; (v) the mixture of peptides (with nitrophenolic marker) is sequenced by tandem MS, a technique which allows for the direct sequencing of peptide fragments at the femtomole level without separation of the mixture.[115]
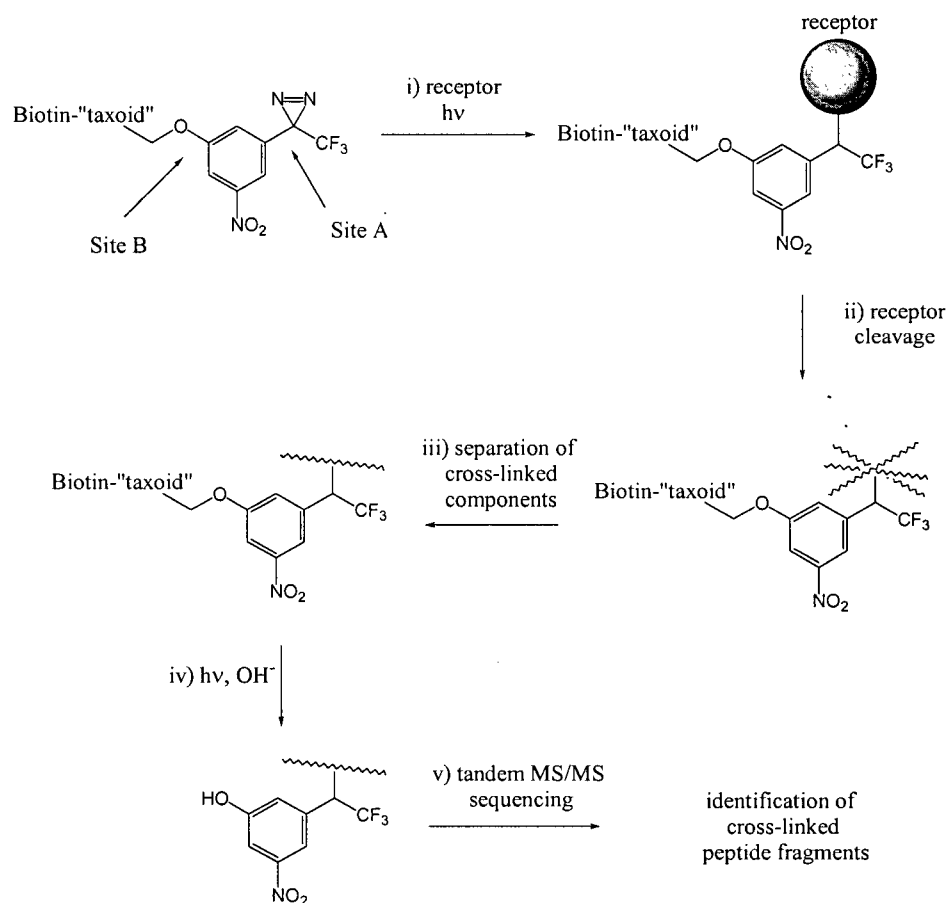
Scheme 1.20. Bifunctional photoactive probe protocol.

The objective of the work presented in this thesis does not involve labeling of a specific binding site, it does however, rely on the mechanism of photoaffinity labeling. It was envisioned to capitalise on the crosslinking ability of both the azido and trifluoromethyldiazarine functionalities in conjunction with the electron/energy transfer capabilities of porphyrins for use in PDT.

1.5 Energy Transfer in Porphyrin Systems Containing a Photoactive Functionality

Desjardins recently reported that the reaction between diazomethane and protoporphyrin dimethylester (70) (PP-DME) gave three pyrazoline-modified porphyrins, two mono-substituted porphyrins [3-substituted (71) and 8-substituted (72)], and one diadduct (73) obtained in the ratio of 1:1:2. (Scheme 1.21).[116]

Exposure of the pyrazoline-modified protoporphyrin to light and/or heat results in extrusion of N_2 and giving a reactive intermediate that could potentially crosslink to biological molecules. Photoextrusion of N_2 from free azoalkanes occurs at wavelengths between 300-400 nm. Pyrazoline-modified protoporphyrins extrude N_2 at 650 nm.[116] The pyrazolines did not chemically crosslink, and only the cyclopropane adducts (Scheme 1.22) were obtained, in high yield, upon thermolysis or photolysis. This type of conversion is typical of pyrazolines.[117] Nonetheless, this result was very exciting, as it was the first instance of a porphyrin fitted with a photo-labile group that could be activated with red light.
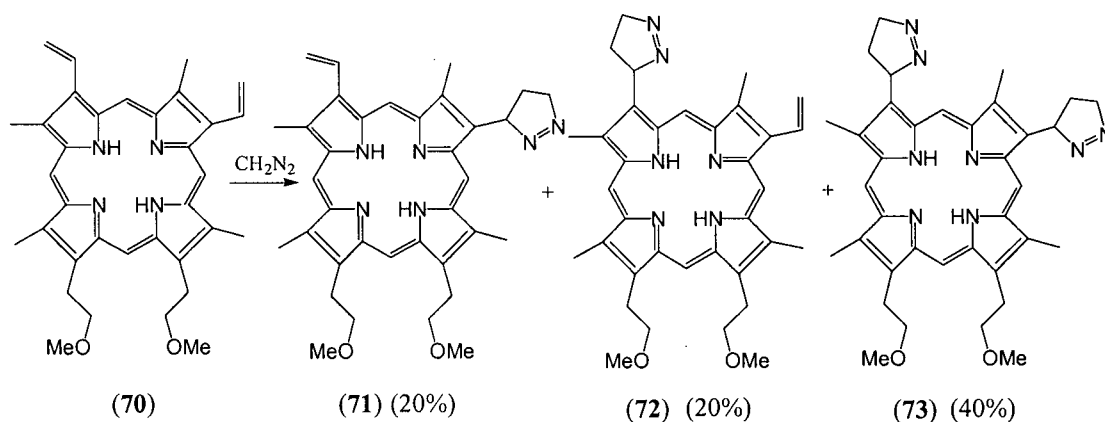
Scheme 1.21. Reaction of diazomethane with PP-DME.
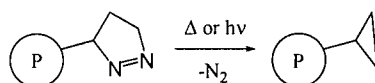
Scheme 1.22. Extrusion of N_2 from pyrazoline-modified porphyrin.

The mechanism of activation in the pyrazoline protoporphyrin is not understood. The respective energy levels of the porphyrin and pyrazoline are such that intermolecular energy transfer is not possible via photosensitization (Figure 1.20). Evidence suggests that the pyrazoline functional group is an integral part of the chromophore, and is intact with the overall electronic structure of the porphyrin.[116] It was hypothesised that in the case of the pyrazoline protoporphyrins, the energy absorbed by the porphyrin at 650 nm (~ 43 kcal/mol) was sufficient to extrude nitrogen from the pyrazoline moeity which has an activation energy (E_a) of 35 kcal/mol. Pyrazolines absorb below 400 nm so the photon at 650 nm is not absorbed by the pyrazoline directly, but by the porphyrin chromophore.[116]
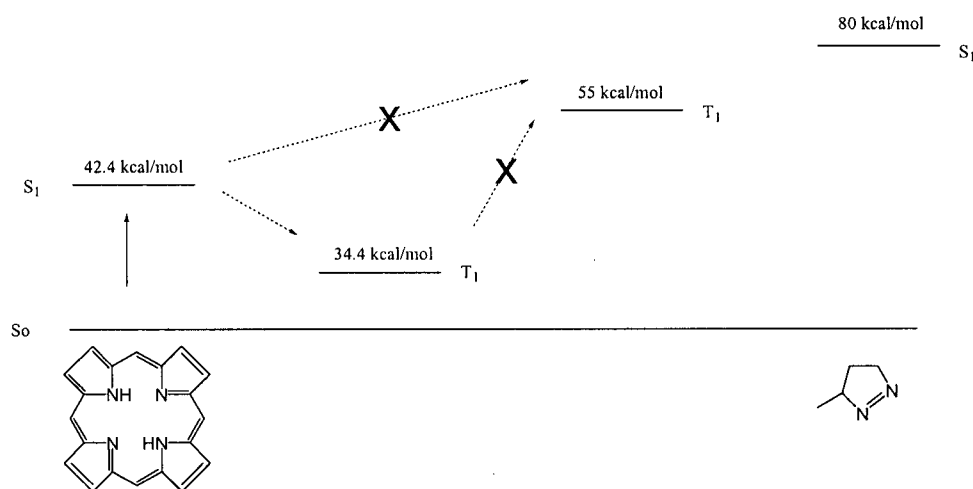
Figure 1.20. Energy level diagram of porphyrin and pyrazoline.

Desjardins observed the same type of activation at 663 nm in a pyrazoline-modified pyropheophorbide (**74**), a chlorin (Figure 1.21).[116]

(74)
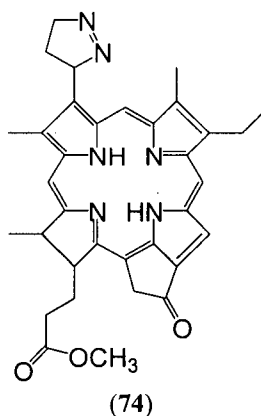
Figure 1.21. Pyrazoline-modified pyropheophorbide.

1.6   Research Objective

Although photosensitizers accumulate preferentially in diseased tissue, they do accumulate in other parts of the body as well.   This can lead to residual skin photosensitivity.   This side effect has led to the investigation of photosensitizers with structural modifications that would allow covalent binding of the drug in the desired area. This could allow for multiple irradiations and potentially lower the drug dosage and be more sparing to healthy tissue. The nature of the porphyrin binding site could be probed using a covalent binding system.

Synthetic targets were designed according to literature precedence based on the ability of the photoactive moiety to be an efficient photo-label, as well as the known sensitising

ability of the porphyrin starting material. As these targets may eventually become commercial PDT drugs, efficient synthesis is imperative for any such target.

This work presents an opportunity to explore the photochemistry involved in activating a crosslinking moiety through absorption of light by the porphyrin chromophore. Each of the successfully modified porphyrins will be activated, both thermally and photochemically. Each compound will be activated in both inert environments and environments where reactive intermediates are likely to undergo C-H insertion or reaction with nucleophiles.

Ideally the molecules would covalently bind to cellular components allowing for 'active selectivity' and new approaches to PDT (Figure 1.22).

Azide modified
photosensitizer

Photosensitizer bound to
cellular component
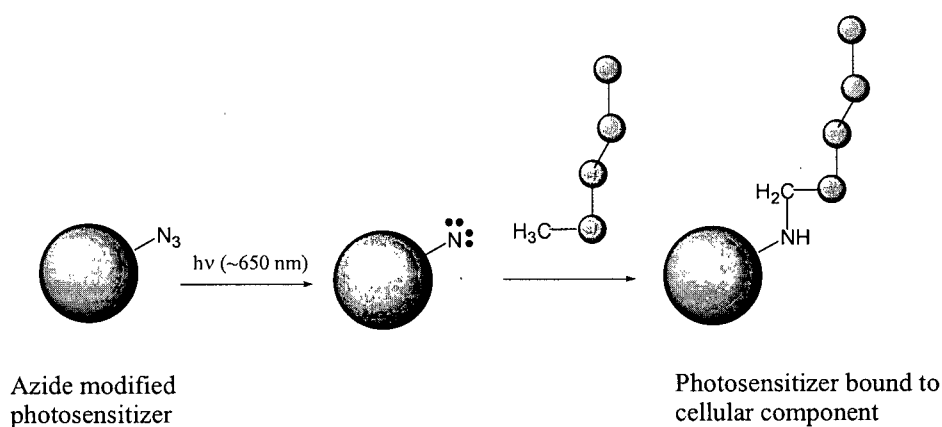
Figure 1.22. Idealised reactivity of an azide-modified photosensitizer.

2 Results and Discussion

2.1 β-Azidomethyl-Tetraphenylporphyrin

2.1.1 Synthesis

Attempts to find other molecules that exhibited similar behaviour to the pyrazoline-modified protoporphyrins (Section 1.5) were investigated. The first target molecule was a novel alkyl azide-modified porphyrin (**77**) shown below.
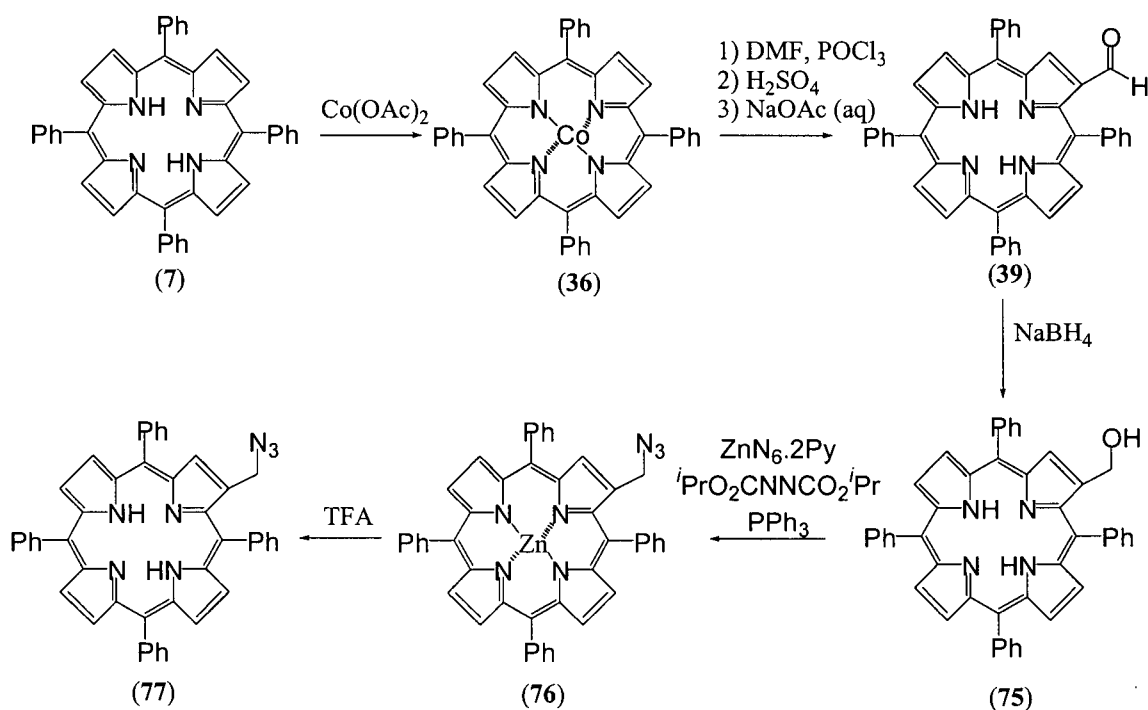
Scheme 2.1. Synthesis of β-azidomethyl-tetraphenylporphyrin.

Metallation of TPP (**8**) with cobaltous (II) acetate affords CoTPP (**36**) in quantitative yield. The method of formylation used was that of Ponomarev[31] as described in Section 1.1.5.1 (Scheme 1.7). Namely, formation of the iminium salt (**37**), demetallation with

H_2SO_4 followed by base hydrolysis. Due to the low solubility of TPP, large amounts of solvent are required. For example, for 500 mg of CoTPP, 300 mL of dichloroethane, followed by 500 mL of H_2O, and 300 mL of benzene were required. Despite the large volumes of solvent required, the reaction does afford the aldehyde (39) in adequate yield (60 %).

Reduction of the formyl group with $NaBH_4$ affords the desired alcohol (75).[31] The reaction gives a single product by TLC, however loss of porphyrinic material is observed during the course of the reaction as yields were on the order of 70 %.

The last step in the sequence was a Mitsunobu reaction.[118] Various primary alcohols have been subjected to Mitsunobu conditions affording high yields of the desired azide.[119] Scheme 2.2 depicts the activation of the primary alcohol (78) with di-isopropyl azodicarboxylate (79) and PPh_3. Nucleophilic substitution with N_3^- (from $ZnN_6{\cdot}2Py$) gives the desired azide (80, Scheme 2.2 and 76, Scheme 2.1) in 85 % yield.
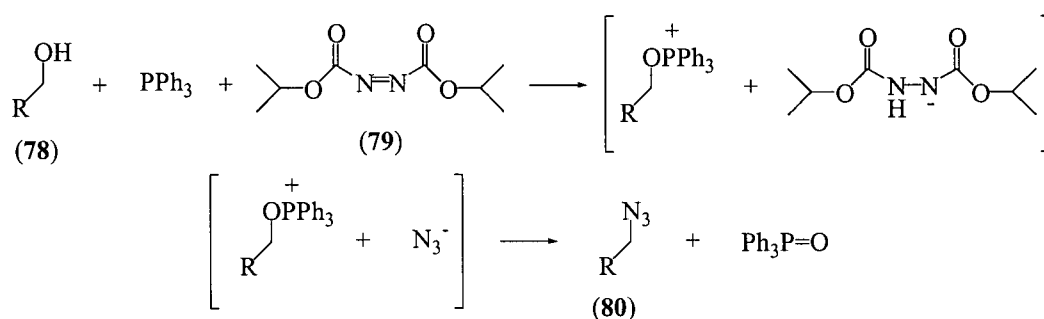
Scheme 2.2. Formation of an alkyl azide under Mitsunobu conditions.

Due to the zinc present in the last step of the sequence (Scheme 2.1), the porphyrin becomes metallated. It is easily removed however with TFA to give **77**. Infrared spectroscopy confirmed the presence of the azido functionality in **76** and **77** by its characteristic asymmetric stretch at 2100 ($\pm$20) cm^{-1}. The ^{1}H-NMR spectra of **77** and its zinc complex are characteristic of mono-substituted (β-position) tetraphenylporphyrins: Signals characteristic of the seven β-protons are observed between δ 9.0 – 8.5 ppm, while signals that correspond to the twenty phenyl protons are observed between δ 8.2 – 7.6 ppm. The signals for the β-**CH$_2$N$_3$** protons are observed at δ 4.65 for **77** and δ 4.50 for its zinc complex. The signals for the inner pyrrole protons of **77** are observed at δ -2.80 ppm. High-resolution mass spectrometry of the zinc complex **76** confirmed the molecular formula C$_{45}$H$_{29}$N$_7$Zn. Microanalysis of **76** was attempted however satisfactory results were not obtained. This was not surprising, as porphyrins frequently do not combust well.

2.1.2 Thermolysis and Photochemistry

Thermal decomposition of alkyl azides without unusual α-substitution commonly requires temperatures that exceed 175°C.[120] This process is generally assumed to proceed via loss of N$_2$ and the generation of an alkyl nitrene, which then rearranges to an imine. (Scheme 2.3)
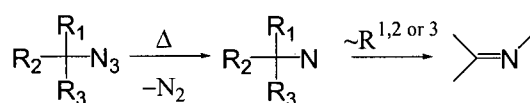
Scheme 2.3. Thermolysis of an alkyl azide.

Thermolysis of **77** in either toluene or mesitylene resulted in one product by TLC (silica). The compound was identified as β-formyl-TPP (**39**, Scheme 2.4) using standard techniques.

Scheme 2.4. Imine formation and subsequent hydrolysis.

It is thought that the imine (**81**) is formed and subsequently hydrolyzed upon purification or exposure to moisture. This was not surprising, as N-unsubstituted imines are known to be unstable and prone to hydrolysis (Scheme 2.4).[121]

It was hoped that compound **77** would exhibit similar photochemical behaviour to that observed with the pyrazoline protoporphyrins. Namely, long wavelength extrusion of nitrogen. In the case of β-azidomethyl-TPP and its zinc complex however, no loss of nitrogen was observed unless wavelengths where the azido group absorbs are used (< 290 nm). This result was disappointing. In both cases, there is no direct conjugation between the porphyrin and the nitrogen-containing group. In the pyrazoline case, there appears to be electronic interaction between the porphyrin and the pyrazoline functionality, thus energy can be effectively shared throughout the entire molecule. Whereas in **77**, the porphyrin and azido group do not interact electronically. Thus, the interaction must be

considered intermolecular in terms of the porphyrin and azide. This means that sensitised photolysis would not be possible due to the respective energy levels. The first triplet energy level of alkyl azides lie at ~77 kcal/mol[122] while the triplet level of the porphyrin is much lower (~35 kcal/mol).

As noted earlier, the energy transfer observed by Desjardins in the pyrazoline-modified porphyrins is not understood.[116] Whether it is a through-space or though-bond phenomenon is not known. The bond being broken in the pyrazoline case is 1 sigma bond away from the porphyrin periphery whereas in **77** it is 2 away. Even though neither group is conjugated directly to the porphyrin, evidence suggests that the CH_2 group in **77** impedes transfer of energy (Scheme 2.5).
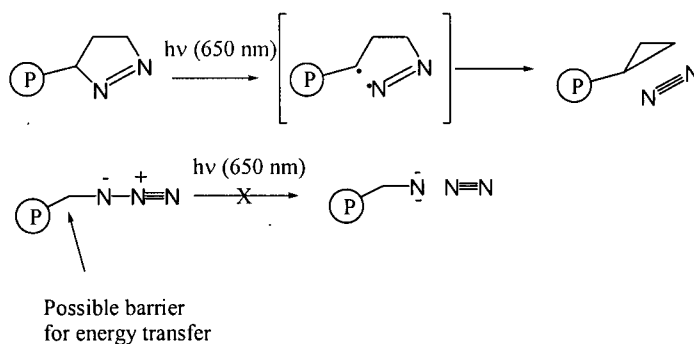
Scheme 2.5. Photochemistry of pyrazoline and alkyl azide-modified porphyrins.

2.2   Progress Towards the Synthesis of *meso*-Azidomethyl-Octaethylporphyrin

Another alkyl azide porphyrin synthesis was attempted via a similar sequence of reactions as shown in Scheme 2.1, the alkyl azide derivative of OEP (**85**) (Scheme 2.6).

Metallation of OEP with CuCl₂ gave CuOEP (**82**) in quantitative yield. Formylation of CuOEP was less efficient (< 50 %) than CoTPP under similar Vilsmeier-Haack conditions. Reduction of the aldehyde (**83**) with NaBH₄ afforded the corresponding alcohol (**84**) as before. However, the Mitsunobu substitution was unsuccessful. A myriad of compounds was observed by TLC, all very close in R_f. None of which were present in particularly high yield or identified as the desired azide (**85**).
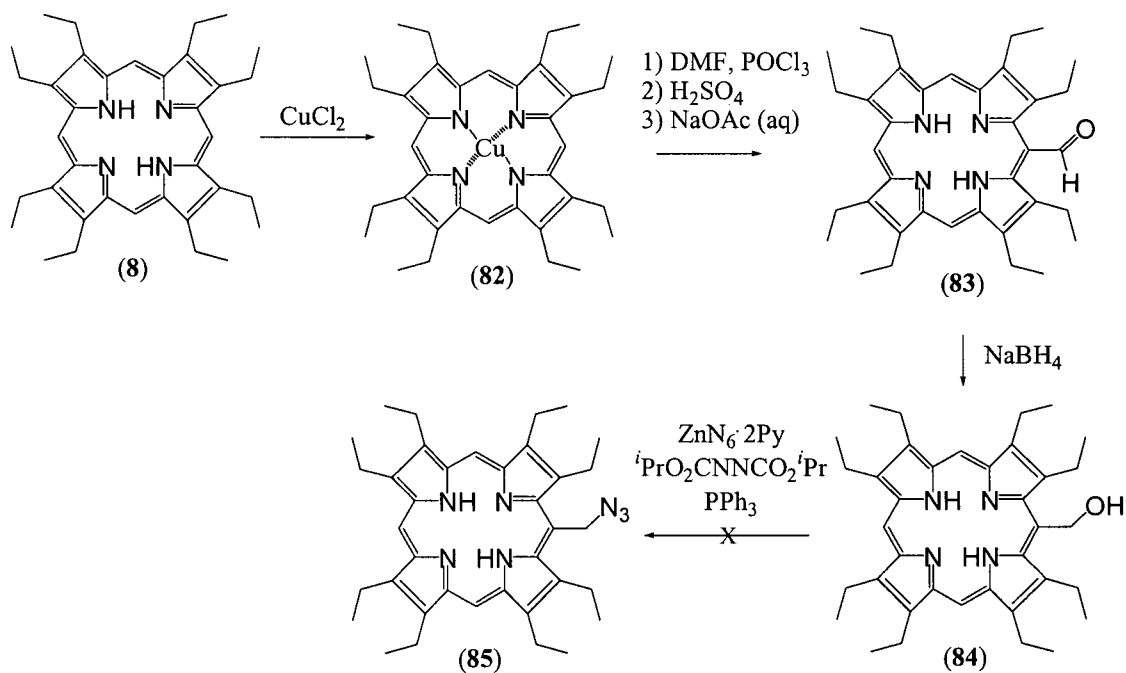
Scheme 2.6. *meso*-Azidomethyl-OEP.

The Mitsunobu substitution failed presumably due to the steric inaccessibility of the *meso*-position in this case. However, since the initial model based on TPP showed no signs of red-light activation it is likely that the OEP derivative would behave similarly.

2.3   β-Azido-Tetraphenylporphyrin

2.3.1   Introduction

As a result of the disappointing photochemical reactivity of **77**, another azide-modified porphyrin was envisioned, namely one where an azide moiety is directly attached to the porphyrin. The tetraphenylporphyrin derivative **86** was chosen and it was necessary to consider viable pathways towards its synthesis. Due to the tautomeric form of the target porphyrin (Figure 2.1) which would have properties similar to both a vinyl and an aryl azide, it was essential to consider the inherent properties of the precursors.
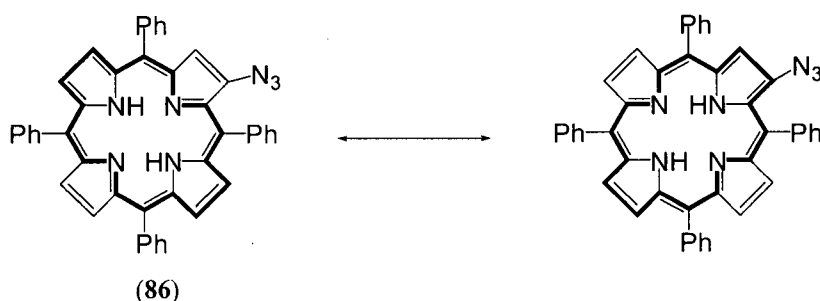
Figure 2.1. Tautomeric forms of β-azido-TPP.

As discussed in the introduction, the most general and widely used method to synthesise aryl azides is diazotization of the corresponding amine followed by addition of sodium azide. This method is usually not applicable to vinyl azides as vinyl amines commonly exist as the imine tautomer, which as noted before, are hydrolytically unstable. Vinyl azides, where the double bond is already present, are commonly synthesised via halide substitution (Scheme 2.7).[88] However, it is necessary to have present an electron

withdrawing group at the β-carbon of the double bond. Unsubstituted porphyrins are electron rich and aromatic, thus halide substitution is unlikely.
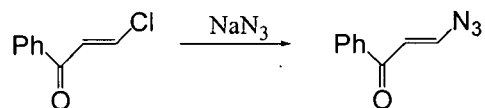
Scheme 2.7. Formation of a vinyl azide.

2.3.2 Synthesis

The synthesis of β-amino-TPP (**90**) from β-nitro-TPP (**89**) has been reported.[123] However β-amino-TPP is known to be an unstable compound.[43] Thus, it was planned to carry out the diazotization on the crude amine immediately after isolation.
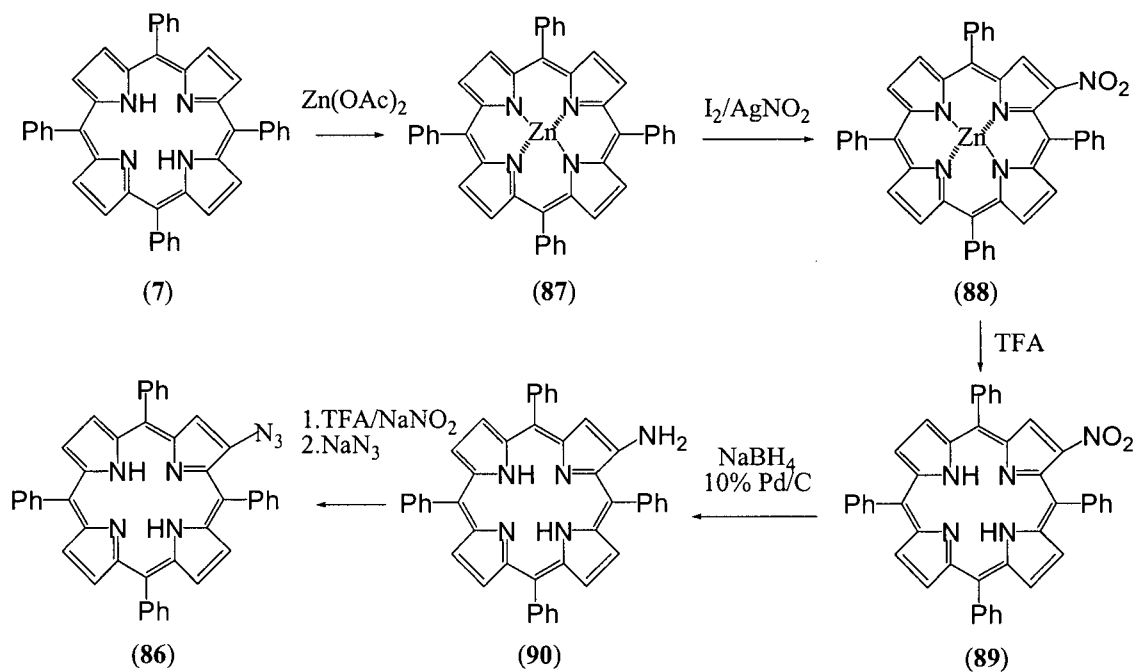
Scheme 2.8. Synthesis of β-azido-TPP.

β-Nitro-TPP (**89**) is easily synthesised as reported,[123] with slight variations. Treatment of ZnTPP with I_2/AgNO$_2$ followed by demetallation with TFA gave β-nitro-TPP (**89**) in 30 % yield. However, the synthesis of the amino derivative (**90**), proved problematic. The literature calls for reduction with NaBH$_4$ with 10 % Pd/C in MeOH/CH$_2$Cl$_2$.[123] It was found that the reported stirring time (45 min) was suspect, as upon working up the reaction mixture, there was very little (< 5 %) porphyrinic material. Diazotization and subsequent treatment with NaN$_3$ was carried out on the reduced material yielding a mixture of compounds. Four major products were formed. The fastest moving spot by TLC was isolated (R$_f$ = 0.75, 60 % CH$_2$Cl$_2$/hexanes). It had a molecular ion (m/z = 656, M+1) corresponding to that of compound **86**. Infrared spectroscopy showed the presence of an absorbance at ~2100 cm^{-1}, which is indicative of the azido functionality. Investigation into the reduction of β-nitro-TPP was carried out in order to increase the yield of the reaction. It was found that the reported stirring time required to reduce β-nitro-TPP was erroneous. Instead of stirring for 45 min, as stated in the literature, the time necessary for reduction to occur was found to be 1-2 min.

The crude amine (**90**) was subjected to diazotization conditions immediately after isolation. There are numerous reported procedures for the diazotization of aryl amines.[124] Many employ the use of strong mineral acids such as HCl (conc.) and H$_2$SO$_4$ (conc.) and then subsequent neutralisation with urea. It was found that employing this type of procedure with porphyrins was not acceptable. Anhydrous diazotization with TFA was found to be ideal in this case.[125] Crude amine (**90**) is readily dissolved in TFA, subsequent diazotization with NaNO$_2$ and treatment with NaN$_3$ yielded the desired azido-

porphyrin (**86**) in high yield (85 % from β-nitro-TPP). Infrared spectroscopy indicated

the presence of an azido group (~2100 cm^{-1}). ^{1}H-NMR spectroscopy gave peaks

indicative of β-substitution on TPP as before and high-resolution mass spectrometry

confirmed the molecular formula $C_{44}H_{30}N_7$ (M+1).

It was discovered accidentally that this material was sensitive to ambient daylight. Upon

preparing a sample for UV-vis spectrometry, the solution changed from light purple to

green within 10 minutes. The UV-visible spectrum changed dramatically as well (Figure

2.2). This led to a variety of photochemical experiments, which will be discussed in the

next section.
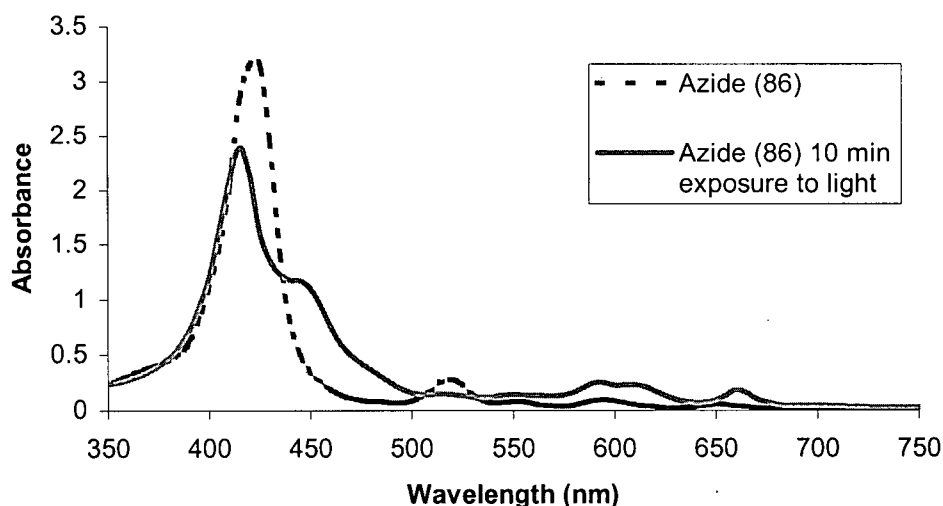
Figure 2.2. UV-visible spectra of β-azido-TPP.

2.3.3 Photochemistry and Modifications

Initially, photochemical experiments were carried out in solvents (THF, CH_2Cl_2, benzene) which were thought to be inert, in that a nitrene would not be likely to under go C-H insertion with the solvent and that the solvent possessed no nucleophilic character. Using CH_2Cl_2 as a reaction solvent proved to be much cleaner than use of either THF or benzene. In dilute solutions (10^{-4} M), photolysis at 650 nm at room temperature took between 30-45 minutes before consumption of the starting material was complete. There was a notable colour change from brown/purple to dark green upon photolysis. Attempts to purify and isolate compounds from the mixture failed. By TLC, the mixture appeared as a green streak with many overlapping components. Mass spectrometry showed peaks that gave little insight to the components of the mixture except that it contained dimeric material (m/z = 1254). High resolution mass spectrometry confirmed the molecular formula $C_{88}H_{58}N_{10}$ of the dimeric material. The pure dimer could not be isolated however it is thought that it may be an azo-type dimer (TPP-N=N-TPP) as this type of reaction is common to nitrenes.[89] Mass spectrometry also showed some (M+16) peaks, indicating oxidation may have taken place. Photolysis was carried out in an oxygen free environment, incorporation of oxygen likely occurred during attempted purification, subsequent to photolysis.

It was thought that some of the photoproducts obtained might be amines. β-Amino-TPP (90) can be acylated with acetic anhydride and pyridine to form the stable acylate as reported by Baldwin.[123] Attempts to acylate the photolysed mixture under similar

conditions to that reported by Baldwin was carried out. Acylation attempts failed and the photolysed mixture appeared unchanged by TLC. Mass spectrometry showed no peaks which indicated that acylation had taken place. Clearly the products formed in such an environment were unstable, therefore attempts to trap the reactive intermediate with a nucleophile were attempted. Photolysis of **86** was attempted in neat diethylamine as diethylamine is commonly used to trap reactive intermediates derived from azide photolysis.[126] Again, the reaction mixture appeared as before, messy and unaffected by the diethylamine. Thermolysis and photolysis of **86** in solvents which nitrenes are known to insert into, such as toluene[104] and mesitylene,[127] were attempted as well but to no avail.

Not only did the products of photolysis/thermolysis of **(86)** appear to be unstable, the reactive intermediate showed no penchant towards nucleophiles. Attempts to trap the intermediate in very dilute solutions (10^{-6} - 10^{-8} M) failed. The results obtained gave no clear indication of the nature of the reactivity of the intermediate.

In an attempt to modify the reactivity of azide **(86)**, metals were complexed with **(86)**. Zinc, copper and cobalt complexes **(91, 92** and **93**, respectively Scheme 2.9) were synthesised and their photochemical behaviour studied. The photochemical behaviour of the zinc complex **(91)** was similar to the free base porphyrin, in that it was extremely light sensitive and products formed upon photolysis were enigmatic mixtures. Mass spectrometry showed 2 major peaks at m/z = 689 (loss of N_2) and m/z = 705 (689 + 16). Again, it appears as if nitrogen loss occurred followed by oxidation. However, as

before, pure compounds could not be isolated from the reaction mixture. Acylation of the photolysis mixture was attempted as before. In this case, the mass spectra contained peaks corresponding to ZnTPP-NHOAc. MS/MS showed a fragmentation pattern consistent with loss of acetate. However by TLC, the mixture appeared as before, a green slur. A variety of solvent systems were used in order to isolate a pure compound. Disappointingly, none could be isolated.
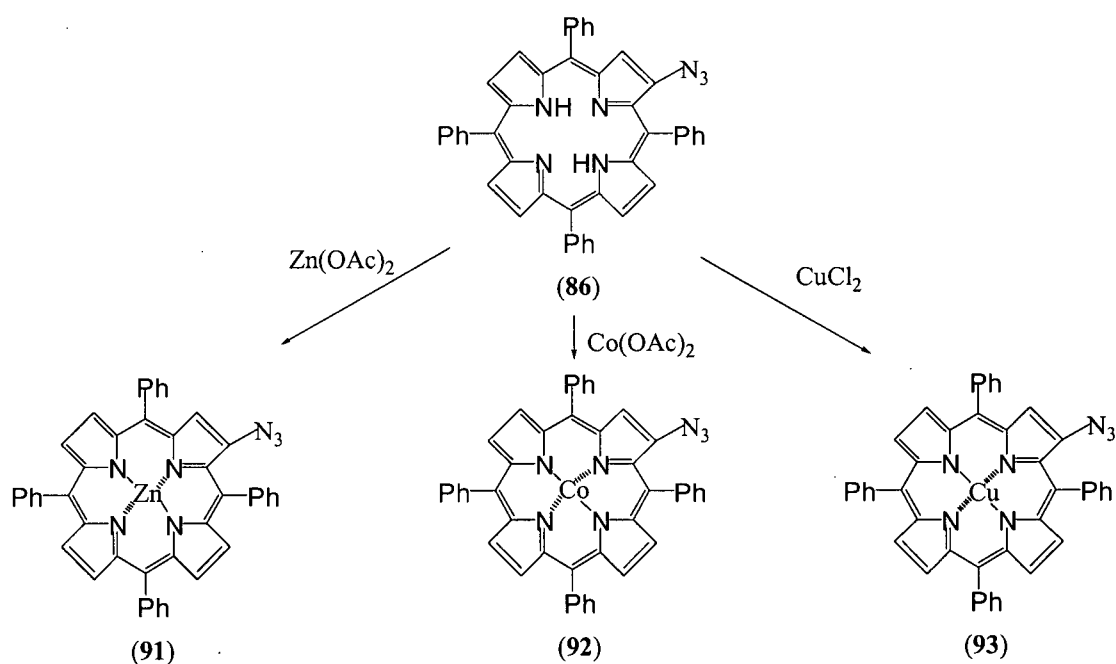
Scheme 2.9. Metallation of β-azido-TPP.

Surprisingly, both the copper and cobalt complexes of **86** were light stable. In order to explain this observation, the electronic nature of both complexes must be considered. Both copper and cobalt porphyrins belong to a group of irregular metalloporphyrins called *hypso*-porphyrins.[48] The irregular metalloporphyrins differ from the regular metalloporphyrins in absorption and emission properties. *Hypso* absorption spectra are

characterised by a blue shift in comparison to normal absorption spectra.[48] This phenomenon is thought to come about via metal to ring π backbonding.[48] Mixing of the LUMO and the HOMO of the porphyrin and metal respectively increases the energy gap between the HOMO and LUMO of the porphyrin, causing a blue shift in the absorption spectrum.[48]

Cobalt porphyrins are known to be radiationless.[48] Various charge-transfer (CT) and (d, d) transitions are thought to be the cause.[48] Copper porphyrins are luminescent at low temperatures, but emission yields are greatly reduced at higher temperatures (> 77 K).[48] This observation is not clearly understood, but it has been suggested that radiationless decay is brought about by some type of CT excited state, which is accessible at higher temperatures.[48] Nickel porphyrins are also *hypso*-porphyrins, however their synthesis involves heating the porphyrin and nickel salt at 80 °C. β-azido-TPP decomposes at temperatures below temperatures required for nickel incorporation.

The properties of the aforementioned porphyrins give some insight to the mechanism of activation seen in **86**. In the presence of metals, which are known to quench radiative processes of porphyrins, extrusion of nitrogen does not readily take place at room temperature. Porphyrins containing paramagnetic metals such as Cu and Co are known to have shorter triplet lifetimes than free-base or zinc porphyrins.[128] Perhaps the activation of the azido group requires energy transfer from the porphyrin triplet excited state. It is also possible that the porphyrin to metal charge transfer processes in Cu and Co porphyrins have effects in centralising the energy absorbed by the porphyrin in the metal,

not allowing for energy transfer to the azido functionality. Whatever the reason, the observed quenching is competing with interchromophore energy or electron transfer.

2.4 Progress Towards the Synthesis of *meso*-Azido-Octaethylporphyrin

The synthesis of *meso*-azido-OEP was attempted via a similar synthetic sequence as (86), namely from *meso*-nitro-OEP (94) → *meso*-amino-OEP (95) → *meso*-azido-OEP (96) (Scheme 2.10).
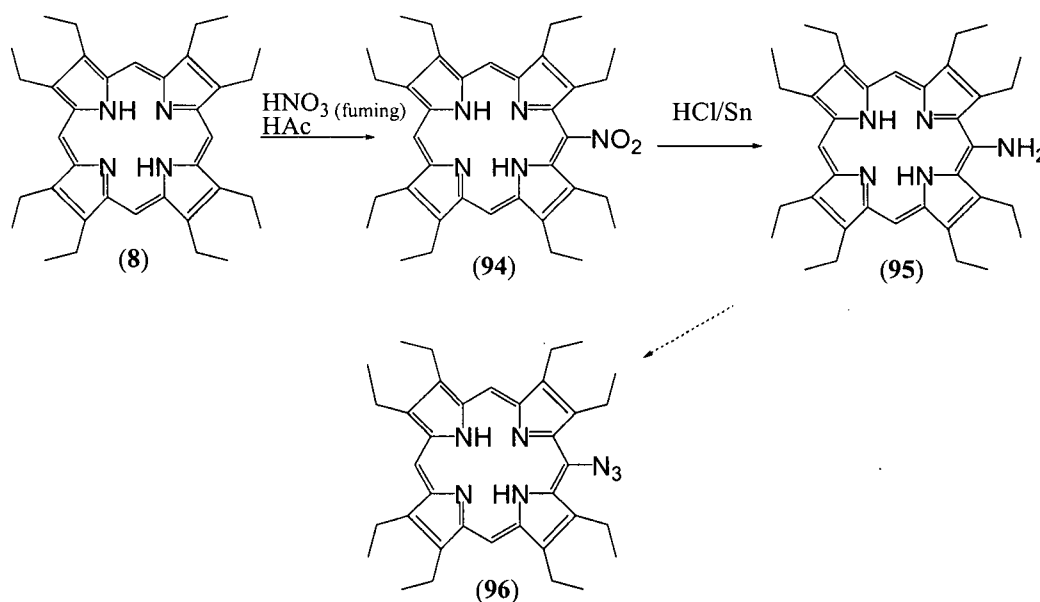
Scheme 2.10. Progress towards azide-modified OEP.

Preparation of both nitro and amino derivatives has been reported in the literature and are both easily synthesised.[129] However, synthesis of the azido derivative (96) proved elusive. *Meso*-amino-OEP (95) was dissolved in TFA, treated with NaNO$_2$ and NaN$_3$. Upon addition of NaN$_3$, violent bubbling was observed. Upon working up the reaction as

before, a complex mixture of compounds was observed by TLC, the major product being *meso*-amino-OEP (**95**). It was unclear if the azide was inherently unstable or even being formed at all. However due to the bubbling observed upon addition of NaN_3 (presumably due to loss o N_2), it appeared as if the azide had formed and immediately decomposed.

Attempts to generate *meso*-azido-OEP (**96**) were carried out at −77 °C. This proved problematic as TFA solidifies at −15°C. A small amount (2 mL) of CH_2Cl_2 was added to liquefy the mixture. $NaNO_2$ was added add the mixture left to stir for 10 minutes. NaN_3 was then added and the mixture was allowed to warm to room temperature. Again, after several minutes, violent bubbling ensued, yet once again a similar mixture containing mostly amino-OEP (**95**) was obtained.

It has been reported that *meso*-aminoporphyrins form diazonium salts using ammonium tetrafluoroborate.[130] Diazotization of *meso*-amino-OEP (**95**) using ammonium tetrafluoroborate instead of TFA gave no reaction.

Iodo-de-diazoniation was attempted in order to prove that the diazonium salt was being formed (Scheme 2.11). However, treatment of the acidified solution (TFA, *meso*-amino-OEP and $NaNO_2$) with KI gave a brownish oily mixture, which contained little porphyrinic material.

$$ArN_2^+ + I^- \rightarrow ArI + N_2$$
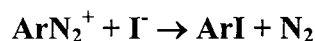
Scheme 2.11. Iodo-de-diazoniation.

2.5 Progress Towards the Synthesis of *meso*-Azido-Diphenylporphyrin

It was hoped that diphenylporphyrin (DPP) might be modified with an azide functionality. Arnold reported on the synthesis of *meso*-nitro-DPP (**98**, Scheme 2.12).[131] He states that attempts to reduce the nitro-group using Baldwin's procedure[123] did not yield the desired aminoporphyrin (**99**).[131] As noted in Section 2.3.2, Baldwin's procedure was found to be in error, in that the mixture of β-nitro-TPP, NaBH₄ and 10 % Pd/C was to be stirred for 45 minutes, while the author (Fenwick) found that the time necessary for reduction was 1-2 min (Scheme 2.8).
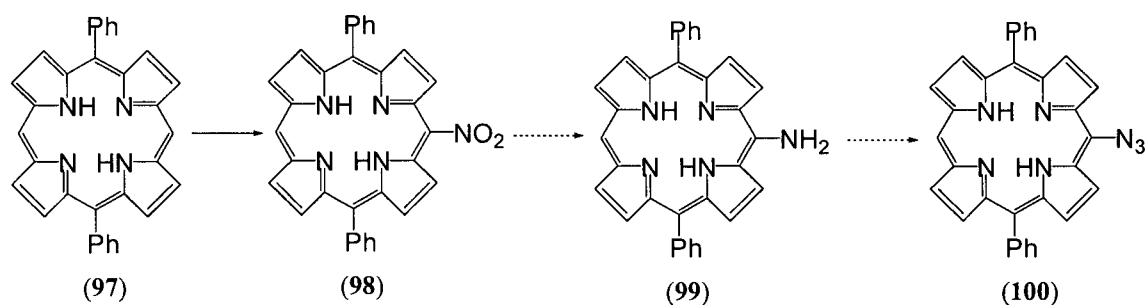
Scheme 2.12. Progress towards azide-modified DPP.

meso-Nitro-DPP (**98**) was synthesised as reported by Arnold.[131] However, reduction, diazotization and treatment with NaN₃ as in the TPP system did not give the desired azidoporphyrin (**99**).

2.6   5-*para*-Azido-Perfluorophenyl-10-15-20-Pentafluorophenylporphyrin

2.6.1   Synthesis

The synthesis of perfluorophenyl azides and the reactivity of pFTPP was discussed in

Section 1.4.2. Based on literature precedent for similar substitutions, it was thought that

pFTPP (**59**) would be able to undergo fluorine substitution with NaN_3. Refluxing pFTPP

(**59**) in acetone and water with NaN_3 afforded 5-*para*-azido-perfluorophenyl-10-15-20-

pentafluorophenyl porphyrin (pFTPP-N_3) (**101**) in 15 % yield.
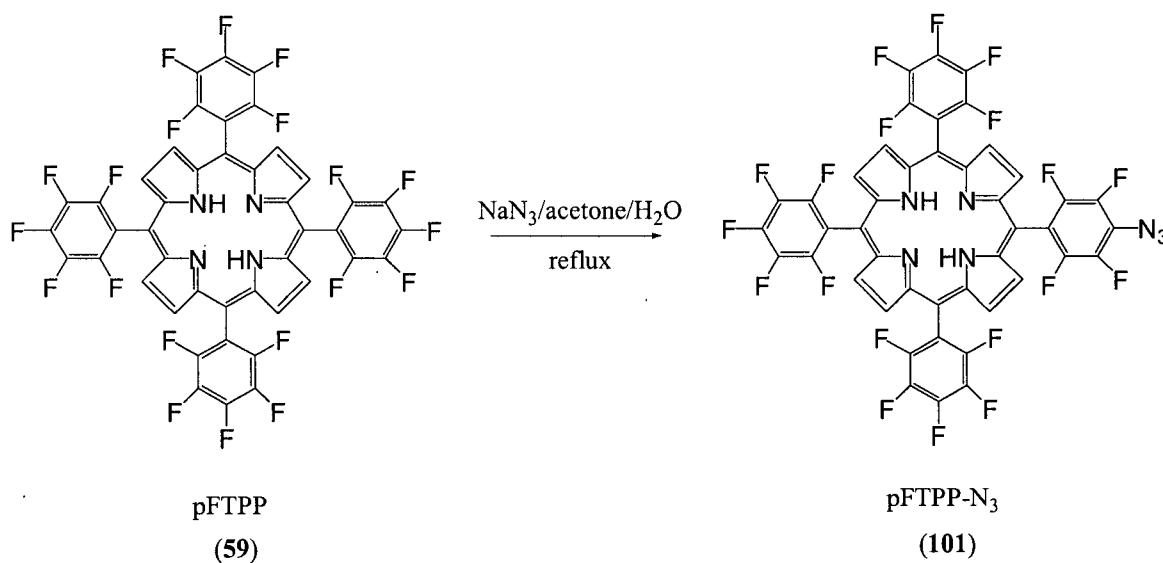
Scheme 2.13. Synthesis of azide-modified pentafluorophenyl TPP, pFTPP-N_3.

Over the course of the reaction, pFTPP is observed as a dark purple spot by TLC and the

formation of new slightly more polar spots, are subsequently formed. The first spot was

identified as **101**. Infrared spectroscopy confirmed the presence of an azido group. [19]F-

NMR was used in order to determine the position of substitution on the phenyl ring. In

fluorine substituted phenyl rings, *ortho*-coupling is reported to be ~20 Hz, *para*-coupling

is ~10 Hz while *meta*-coupling is ~2 Hz.[132] Figure 2.3 shows the ^{19}F-NMR spectrum of

101 and clearly shows a splitting pattern consistent with *para*-substitution. High

resolution mass spectrometry confirmed the molecular formula $C_{44}H_{11}N_7F_{19}$ (M+1).
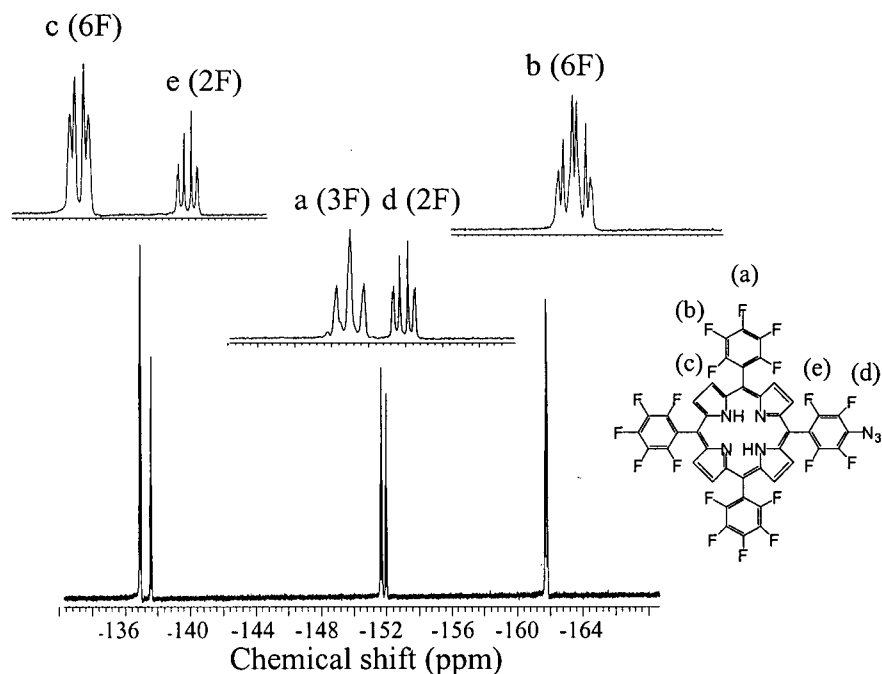
Figure 2.3. ^{19}F-NMR spectrum of (**101**).

The second spot was identified as a di-azido-pFTPP (**102**) (Figure 2.4). ^{19}F-NMR spectral

data showed that substitution had taken place on another phenyl ring at the *para*-position.

Five sets of peaks were observed, one integrating for two F-atoms the other 4 integrating

for 4 F-atoms each. ^{1}H-NMR spectral data showed a symmetrical doublet at δ 8.9 ppm

indicating that substitution had taken place on the opposite phenyl ring. Mass

spectrometry confirmed the presence of the molecular ion m/z = 1021 (M+1) as well as

m/z = 993 (M-28) and m/z = 965 (M-56) consistent with loss of N_2 and 2 x N_2,

respectively.

(102)
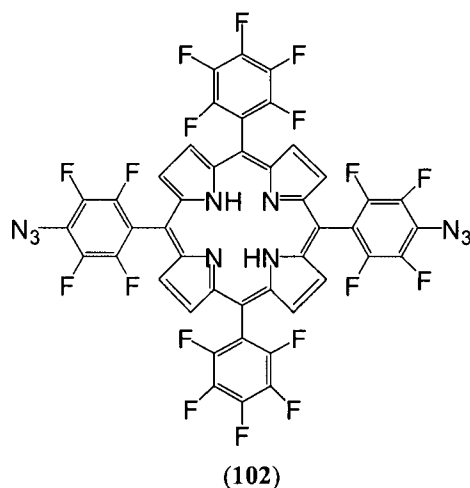
Figure 2.4. Di-azido-pFTPP.

The electronegativity of N_3^- is reported to be between that of I^- and Br^-, and like the halogens, N_3^- is capable of electron donation through its non-bonding electrons.[133] This inductive effect increases the electron density in the phenyl group in which it belongs and makes further substitution on the same ring unlikely. If instead of N_3^-, electron withdrawing substituents such as CN^- are introduced at the *para*-position, further substitution occurs on the same phenyl ring.[110] This is due to the fact that the cyano-substituted phenyl ring has become more electron deficient than the other phenyl rings thus more susceptible to nucleophilic attack. However, if electron donating groups such as alkoxides or amines are used, substitution on the same phenyl ring becomes less likely.[110]

Unfortunately, introduction of the azido group into pFTPP did not markedly alter the UV-visible spectrum suggesting that the azido group was not interacting electronically with the porphyrin chromophore. Nevertheless photochemical and thermolysis reactions were

carried out in order to study the nature of the reactive intermediate brought about by extrusion of nitrogen from **101**.

2.6.2 Thermolysis and Photochemistry

As noted earlier, perfluorophenyl azides are known to insert into toluene. Photolysis of **101** in toluene at 350 nm for 48 h gave the corresponding amine (**103**) in low (5-10 %) yield and starting material (70 %) (Scheme 2.14). Thermolysis of **101** in toluene gave similar results. Over the course of the thermolysis the amine (**103**) could be seen by TLC. However, if the mixture was left to reflux for > 48 h, much of the material became tar-like and resided on the baseline of a silica plate during chromatography.
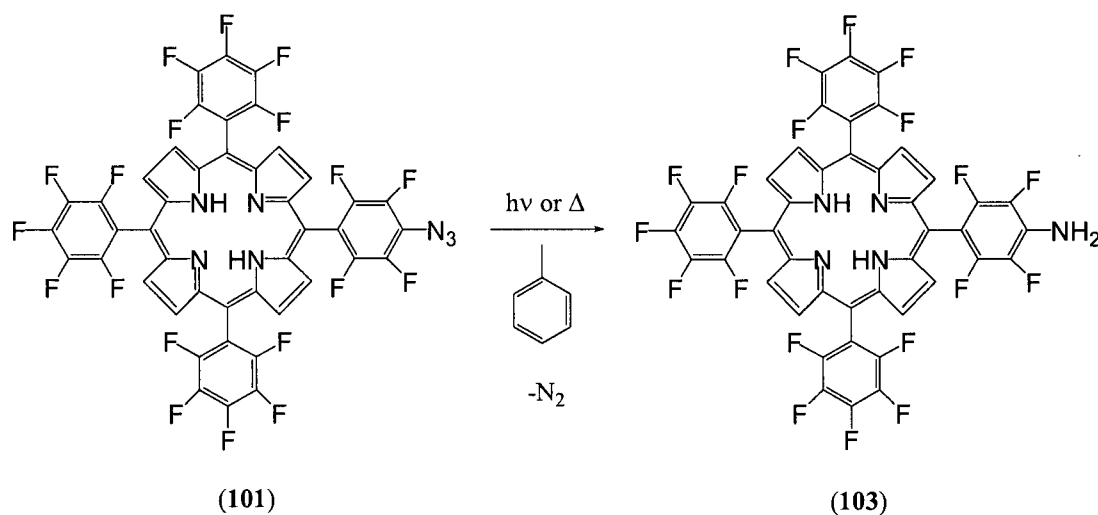
Scheme 2.14. Thermal and photochemical reactivity of (**101**) in toluene.

In toluene, activation of **101** promoted the formation of triplet products. No toluene C-H insertion was observed and photolysis of **101** with red light (600 nm) gave no reaction.

Thermolysis was carried out in a higher boiling and more nucleophilic solvent, namely mesitylene, in which nitenes[127] and nitrenium[134] ions have both been reported to insert. Thermolysis in mesitylene yielded a singlet nitrene derived product (104) in 40 % yield (Scheme 2.15).
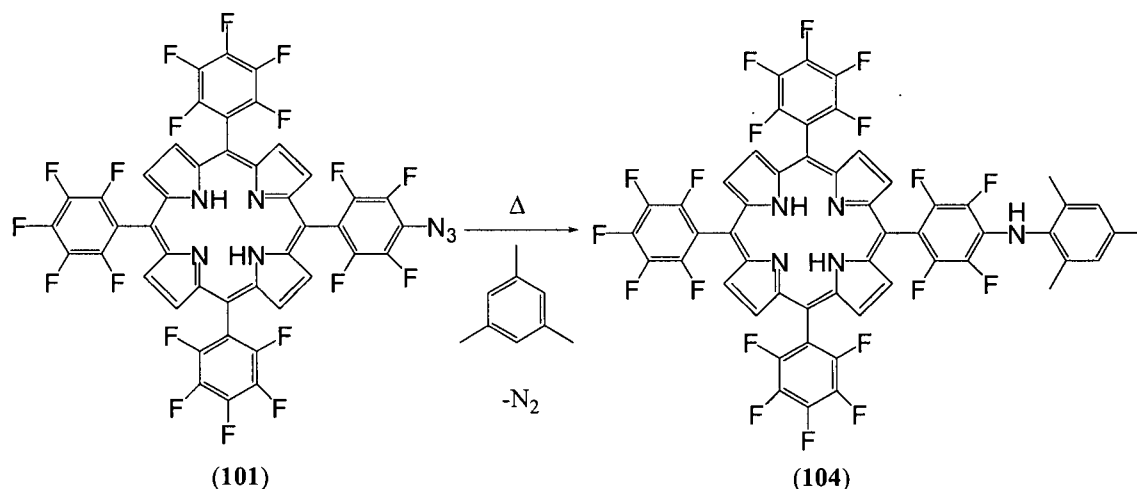
Scheme 2.15. Thermolysis of (101) in mesitylene.

In addition to peaks corresponding to the β-protons and inner pyrrole protons, the ^{1}H-NMR spectrum of **104** showed the following peaks: a singlet at δ 7.02 ppm corresponding to the two aromatic protons of the mesityl group, a broad singlet at δ 5.69 ppm (NH) as well as two singlets at δ 2.49 ppm (6H) and δ 2.35 ppm (3H). High resolution mass spectrometry confirmed the molecular formula $C_{53}H_{23}N_5F_{19}$ (M+1).

As in the case of toluene, some baseline and tar-like material is observed by TLC. In addition to **104** a faster moving green spot is also observed by TLC. This green material appeared to be chlorin-like in nature as the UV-visible spectrum showed an intense peak

at ~650 nm, not observed in the UV-visible spectra of **104** or any other precursors. Mass

spectrometry of the green component showed 2 major peaks of higher molecular weight

than **104** (m/z = 1091) differing in weight by one or two mesitylene units (m/z = 1211

and 1329). NMR did not give clear insight as to the components of the mixture.

It is unclear as to why electron/energy transfer from the porphyrin to the azido group was

not possible, or inefficient at best in this instance. Clearly the porphyrin interacts

electronically with the phenyl groups, as the UV-visible spectrum of pFTPP is markedly

different from that of TPP (Figure 2.5). However, this may be the result of an inductive

effect as the phenyl rings are essentially orthogonal to the porphyrin. This non-planarity

may hinder π-delocalisation.
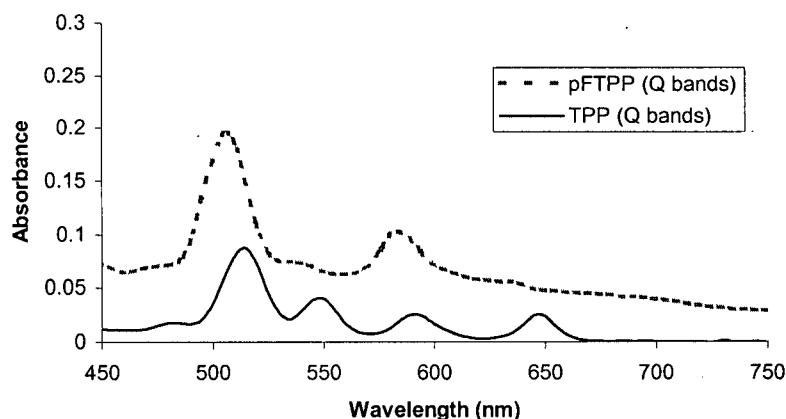
Figure 2.5.   UV-visible spectra of TPP and pFTPP.

Even though red light activation was not possible in this case, the synthesis of a novel

azido-modified porphyrin was achieved and this is the first instance in which a porphyrin

has been fitted with an azide that has shown the ability to insert.

2.7 Progress Towards the Synthesis of Diazirine-Modified Porphyrins

Previous work in the Dolphin lab included attempts at the synthesis of a diazirine-modified porphyrin. The chosen synthetic route is shown in Scheme 2.16. It was reported by Desjardins[116] that the trifluoroacetyl-modified TPP (106) was synthesised in high yield (> 80 %). However, formation of the oxime (107) was only achieved on one occasion by Desjardins and the reported yield of 60 % is highly suspect. Tosylation was never achieved.
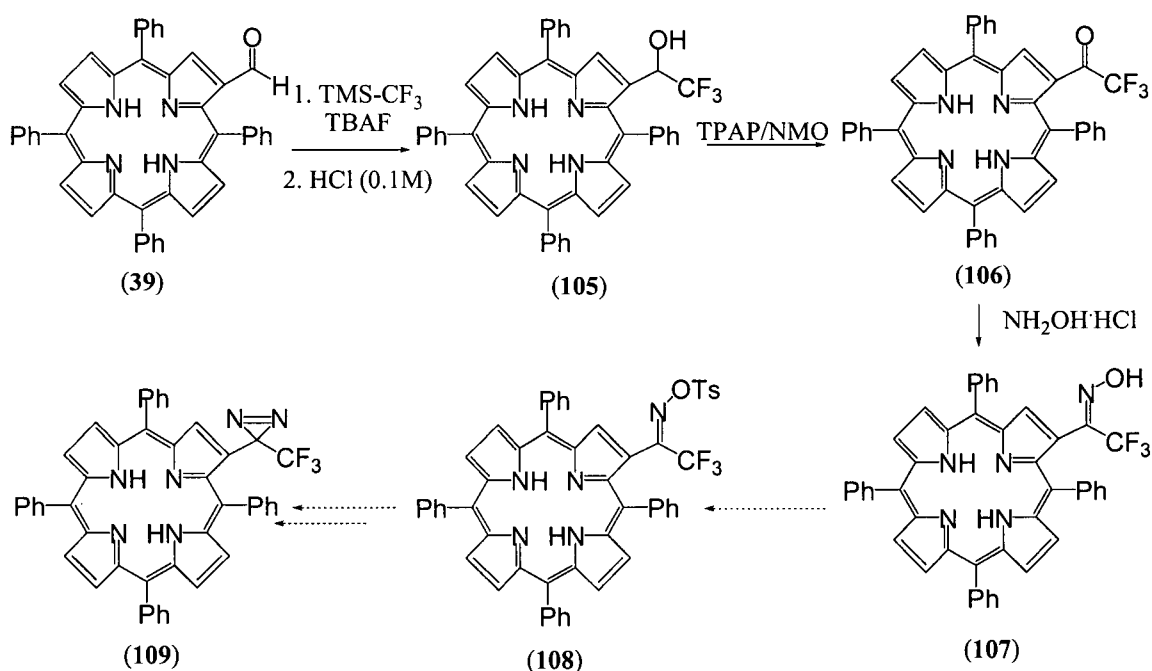
Scheme 2.16. Progress towards the synthesis of Diazirine-modified TPP.

The author was able to synthesise 106 as reported. However, formation of the oxime (107) proved difficult. It was reported that refluxing 106 in benzene with activated 7Å molecular sieves gave 107 in 60 % yield.[116] It is thought that the reported use of 7Å

molecular sieves is erroneous, as no such sieves were found in the Dolphin lab or in commercial catalogues. Under similar conditions (refluxing in benzene with 5 Å or 3 Å sieves) yielded **107** in no more than 10% yield. Due to the formation of water during the course of the reaction, it was thought that use of a Dean Stark trap might increase the yield. However, use of the Dean Stark trap did nothing to increase the yield.

Literature methods for formation of an oxime in similar systems, i.e., R-CNOHCF$_3$ from R-COCF$_3$ and NH$_2$OH·HCl involve use of ethanol/pyridine solvent mixtures.[135] No reaction was observed when these systems were employed.

The small amount of **107** obtained was treated with TsCl in pyridine, as reported in the literature.[136] However, no tosylated material was obtained. Due to the inefficiency in which the oxime is formed, tosylations were only attempted a small number of times, none of which were successful. It is not understood why a seemingly simple reaction is not applicable in this porphyrin system.

The synthesis of a diazirine-modified OEP (**111**) was also attempted (Scheme 2.17). However, only two steps of the sequence were carried out due to time constraints and low yields.
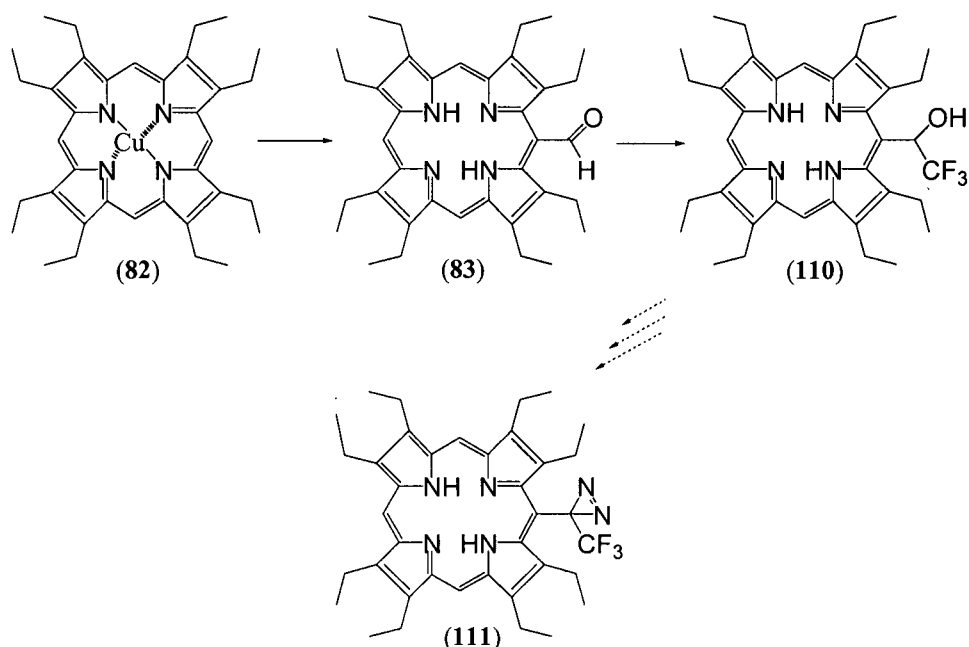
Scheme 2.17. Progress towards diazirine-modified OEP.

3 Conclusions and Suggestions for Further Studies

In this thesis, the synthesis, isolation, characterisation and reactivities of three novel azide-modified porphyrins (**77**, **86** and **101**) were described. In **77**, extrusion of N_2 was only possible with heat and high energy light ($\lambda < 290$ nm). Activation led to loss of N_2, and formation of **39**. In **86** extrusion of N_2 was possible with heat and red light ($\lambda = 650$ nm). The thermolysis/photolysis mixtures obtained were enigmatic mixtures in which pure compounds could not be isolated. In **101** extrusion of N_2 occurred with heat and inefficiently at $\lambda = 350$ nm. Two nitrene derived products were obtained, the triplet derived (**103**) and the singlet derived (**104**).

It would be ideal to combine the properties of **86** and **101**, namely create a porphyrin/azide system which is activatable with red light and has the ability to insert into C-H bonds.

It was disappointing that a diazirine-modified porphyrin was not synthesised during the course of this work. It would have been interesting to see if the diazirine moiety could be activated with red light and chemically cross-linked. In order to overcome the problems of oxime formation, perhaps instead of using $NH_2OH \cdot HCl$, an amine modified with an organic group could be used (Scheme 3.1). This would increase solubility and lower the number of steps in the sequence.

(106)   (112)

X = organic leaving group
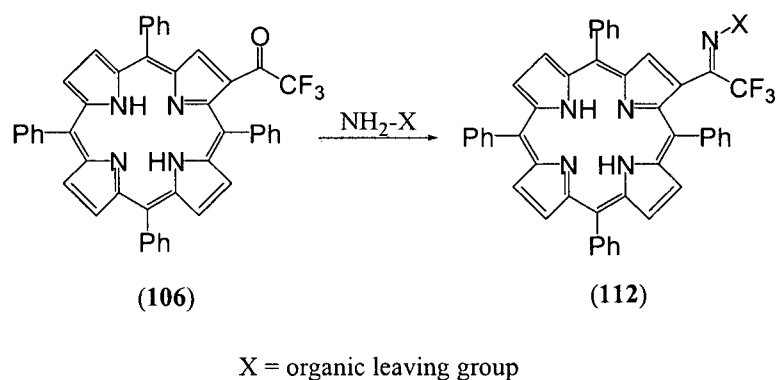
Scheme 3.1. Imine formation with modified amine.

4 Experimental

4.1 Instrumentation and Materials

Mass Spectrometry (MS)

Mass spectrometric analyses were carried out by the author, or by staff at The B. C. Regional Mass Spectrometry Centre at the University of British Columbia, Department of Chemistry. Technicians carried out low and high resolution mass spectra by liquid secondary ion mass spectrometry (LSIMS) on a KRATOS Concept IIHQ hybrid mass spectrometer. Low resolution electrospray ionisation spectrometry (ESI) were carried out on a Bruker Esquire liquid chromatography mass spectrometer by the author. High resolution ESI spectra were carried out by technicians on a Micromass LCT, HPLC-TOF mass spectrometer. Molecular ions are designated as (M+1).

UV-visible Spectrophotometry

UV-visible spectra were measured on a Cary 50 spectrophotometer. Wavelengths for each absorption maximum (λ_{max}) are reported in nanometers.

Infrared Spectroscopy (IR)

Infrared spectra were recorded using a Perkin Elmer model 1600 Fourier Transform infrared spectrometer with internal calibration. Spectra were recorded as KBr pellets.

Nuclear Magnetic Resonance Spectroscopy (NMR)

NMR spectra were recorded either by the author, by Marietta Austria or Liane Darge of the University of British Columbia Department of NMR Service Laboratory.

^{1}H-NMR Spectroscopy

Proton nuclear magnetic resonance spectra (^{1}H-NMR) were recorded on the following spectrometers: Bruker WH-400 (400 MHz) and Bruker AV-300 (300 MHz). The positions of the signals are given as chemical shifts (δ) in parts per million (ppm) with respect to tetramethylsilane (TMS) at δ 0 ppm; however, the internal reference standard in each case was the residual proton signal present in the deuterated solvent. The multiplicity of the peak, the coupling constant in Hz and the number of protons follow reported chemical shifts in parentheses.

^{19}F-NMR Spectroscopy

Fluorine nuclear magnetic resonance spectra were recorded on the AV-300 spectrometer. The positions of the signals are given as chemical shifts (δ) in parts per million (ppm) with respect to trifluoroacetic acid (TFA) at δ 0 ppm.

Chromatography

Chromatographic separations were carried out using silica gel 60, 70-230 mesh, supplied by E. Merck Co. Thin layer chromatography (TLC) was carried out on pre-coated silica plates (Merck 60, 230-400 mesh, with aluminum backing). Preparative thin layer

chromatography was performed on pre-coated 10 x 10 cm 0.5 or 1mm thick Merck silica gel plates.

Elemental Analyses

Micoroanalyses were carried out in the microanalytical laboratory in the Department of Chemistry, University of British Columbia by Mr. Peter Borda using Carlo Erba Elemental Analyzer 1106. Satisfactory results were not obtained presumably due to inefficient combustion of the porphyrins.

Reaction Conditions

Due to the inherent light sensitivity of porphyrins, all reactions were performed in a dark fumehood and reaction flasks surrounded by aluminum foil. All glassware was flame-dried and reactions were performed under N_2 unless noted otherwise.

Reagents and Solvents

Unless otherwise specified, reagents were used as supplied by the Aldrich chemical company. Porphyrin starting materials were obtained from Strem or Porphyrin Products. Solvents were of reagent or HPLC grade and purified using standard literature methods when necessary. Deuterated solvents were supplied by Cambridge Isotope Laboratory.

Photochemical Studies

Photochemical irradiations were carried out with either a 250W Osram HLX 64655 arc lamp in an Oriel housing, a rayonette Photochemical Chamber Reactor (Model RPR-100)

or a quartz (λ > 190nm) filtered light from a Hanova 450 watt medium pressure mercury lamp. The light output from the Oriel lamp passed through a glass filter: P70-650-S-533G-Corion or P70-600-S-533G-Corion when necessary.

4.1.1 Metallation of Porphyrins (Large Scale, ~500 mg)

The desired porphyrin (TPP or OEP) was dissolved in $CHCl_3$ in a 1:1 mg/ml ratio (500 mg/500 mL). A saturated solution of the appropriate metal salt (cobaltous (II) acetate, zinc (II) acetate or copper (II) chloride) in methanol (2 mL) was added to the porphyrin solution. The solution was refluxed for 1 h, evaporated to dryness and the product extracted from CH_2Cl_2.

4.2 Preparation of β-Azidomethyl-TPP (77)

β-Formyl-TPP (39)

(39)
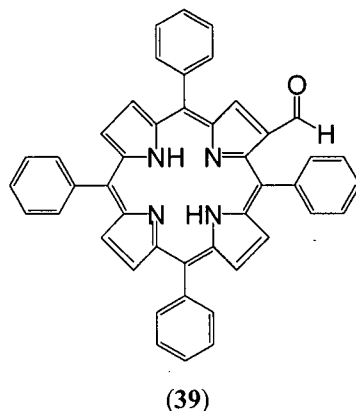
β-Formyl-TPP (28) was synthesised as reported by Ponomarev,[31] with slight modifications. $POCl_3$ (2.25 mL, 24.1 mmol) was added to a 2 L round bottom flask and cooled to 0 °C. DMF (1.90 mL, 24.2 mmol) was then added and the contents were

allowed to warm to room temperature and left to stir for 60 min. A solution of CoTPP

(500 mg, 0.74 mmol) in dichloroethane was added to the clear bright yellow solution and

the reaction mixture was heated at 60 °C for 30 min.

The solvent was then evaporated under reduced pressure, and 500 mL of cold H_2O was

added rapidly to the green residue. After 10 min, filtering the water through a coarse

sintered glass fritted filter collected the precipitate. The precipitate was then returned to

the original 2 L flask and dissolved in 10-15 mL of conc. H_2SO_4 and stirred for 1 hour (1-

2 mL of acid was run though the fritted filter into the 2 L flask as to dissolve and residual

precipitate on the filter).

A saturated aqueous sodium acetate solution (500 mL) was added slowly to the acidified

mixture until a neutral pH was observed. Additional sodium acetate was added if the

solution was still acidic. Benzene (300 mL) was added to the flask and the mixture was

allowed to reflux for 1 h. The organic layer was separated from the aqueous layer, passed

through alumina (activity 3) and evaporated to dryness. The residue was purified by

chromatography on silica. The dark green band (R_f = 0.65, 30 % CH_2Cl_2/hexanes) was

collected as a purple solid (285 mg, 60 %). UV-vis (CH_2Cl_2) λ_{max} (rel. intensity): 430

(1), 526 (0.07), 567 (0.03), 606 (0.03), 662 (0.03). I.R. (KBr) 1672 cm^{-1} ($\nu_{C=O}$). ^{1}H-NMR

(300 MHz, CDCl$_3$, ppm) δ 9.46 (s, 1H), 9.24 (s, 1H), 8.92 (m, 4H), 8.82 (s, 2H), 8.23 (m,

8H), 7.77 (m, 12H), -2.5 (s, 2H). LRMS (LSIMS) m/z: 642 (M+1).

β-Hydroxymethyl-TPP (75)

(75)
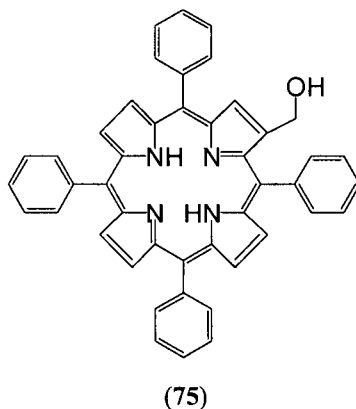
A 50 mL round bottom flask was charged with β-formyl-TPP (200 mg, 0.3 mmol). THF (40 mL) was added and the solution stirred for 10 min. NaBH$_4$ (333 mg, 8.8 mmol) was added to the flask, and the mixture was heated at 50°C. The reaction was monitored by TLC and stopped when the starting material was completely consumed (10-15 min). The solvent was evaporated to dryness and the product was extracted from CH$_2$Cl$_2$ yielding the dark purple solid (75, 140 mg, 70 %) which was used without further purification. R$_f$ = 0.6 (silica, 100% CH$_2$Cl$_2$). UV-vis (CH$_2$Cl$_2$) λ_{max} (rel intensity): 420 (1), 515 (0.06), 550 (0.02), 590 (0.02), 645 (0.02). ^{1}H-NMR (300 MHz, CDCl$_3$, ppm) δ 8.93 (s, 1H), 8.80 (m, 5H), 8.59 (d, J = 4.79 Hz, 1 H), 8.20 (m, 6H), 8.08 (m, 2H), 7.74 (m, 12H), 4.98 (s, 2H), -2.80, (s, 2H). LRMS (LSIMS) m/z: 644 (M+1).

ZnN$_6$2Py

ZnN$_6$2Py was synthesised according to literature methods.[119] To a stirred 2 M aqueous solution of Zn(NO$_3$)$_2$ (20 mL, 40.0 mmol) is added dropwise a 2 M aqueous solution of NaN$_3$ (40 mL, 80.0 mmol). The white suspension is heated to 50 °C, then a slight excess

of pyridine (6.67 mL, 82.3 mmol) is added dropwise causing the solution to turn light pink. Stirring was continued and the solution was cooled to room temperature resulting in the formation of a dense white precipitate. The salt is filtered, washed with ice-cold water and dried *in vacuo* for 24 h behind a blast shield to give a white crystalline powder (9.1 g, 74%).

β-Azidomethyl-TPP (77) and β-Azidomethyl-ZnTPP (76)

(76)   (77)
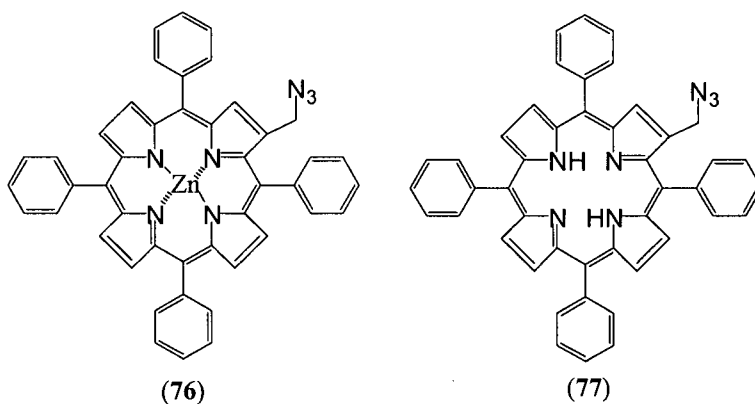
ZnN_6 2Py (0.46 g, 1.5 mmol) was suspended in a solution of β-hydroxymethyl-tetraphenylporphyrin (80 mg, 0.124 mmol) and Ph_3P (1.05 g, 4 mmol) in dry toluene. To this stirred mixture at room temperature is added di-isopropylazodicarboxylate (0.8 mL, 4 mmol) dropwise. The reaction mixture was left to stir for 12 h. The crude mixture was purified by column chromatography on silica gel (70 %, CH_2Cl_2/hexanes). The zinc complex (76) was observed as a pink/purple spot at $R_f = 0.7$ (70 %, CH_2Cl_2/hexanes) obtained in 85 % yield (77 mg). The zinc complex (76) was then dissolved in 3-5 mL of trifluoroacetic acid and stirred for 1 h. The mixture was neutralised with ice water and

aqueous sodium acetate then extracted with CH_2Cl_2. The mixture was dried *in vacuo* yielding the pure product **77** in quantitative yield from **76**.

β-Azidomethyl-ZnTPP (76): UV-vis (CH_2Cl_2) λ_{max} (rel. intensity): 420 (1), 548 (0.06), 586 (0.01). I.R. (KBr): 2098 cm^{-1} (v_{N_3}). ^{1}H-NMR (300 MHz, CDCl$_3$, ppm) δ 8.95 (m, 6H), 8.73 (d, J = 4.64 Hz, 1H), 8.20 (m, 6H), 8.09 (br d, 2H) 7.65 (m, 12H), 4.50 (s, 2H). HRMS (LSIMS) dev. in ppm for mass calculated for C$_{45}$H$_{29}$N$_7$Zn: -0.16, found 731.17742 m/z (^{64}Zn) (M+1).

β-Azidomethyl-TPP (77): UV-vis (CH_2Cl_2) λ_{max} (rel. intensity): 420 (1), 515 (0.05), 550 (0.02), 590 (0.02), 650 (0.03). I.R. (KBr): 2098 cm^{-1}(v_{N_3}). ^{1}H-NMR (300 MHz, CDCl$_3$, ppm) δ 8.83 (m, 6H), 8.65 (d, J = 4.83 Hz, 1H) 8.20 (m, 6H), 8.11 (m, 2H), 7.74 (m, 12H) 4.65 (s, 2H), -2.80 (s, 2H). LRMS (ESI) m/z: 670 m/z (M+1).

Thermolysis of (76) and (77)

20 mg of the appropriate porphyrin (**76**) or (**77**) was dissolved in dry toluene (20 mL), stirred and heated to reflux for 12 h. The crude product was purified by preparatory TLC (silica, 70 % CH_2Cl_2/hexanes for **77**, 100 % CH_2Cl_2 for **76**) and identified as β-formyl-TPP (**39**) (9-10 mg, ~50 %), or the zinc complex thereof (9-10 mg, ~50 %).

Photolysis of (76) and (77)

10 mg of the appropriate porphyrin was placed in a quartz tube and dissolved in dry THF (10 ml) and degassed with N_2. The mixture was photolysed at < 290 nm for 3 h. The

product was purified by preparatory TLC (silica, 70 % CH₂Cl₂/hexanes for **76**, 100 %

CH₂Cl₂ for **77**) and identified as formyl-TPP (**39**) (9-10 mg, ~50 %), or the zinc complex

thereof (9-10 mg, ~50 %).

β-Formyl-ZnTPP : R_f = 0.4 (100% CH_2Cl_2) UV-vis (CH_2Cl_2) λ_{max} (rel. intensity): 420

(1), 548 (0.06), 588 (0.01). I.R (KBr): 1672 cm⁻¹($\nu_{C=O}$). ¹H-NMR (300 MHz, CDCl₃,

ppm) δ 9.54 (s, 1H), 8.28 (s, 1H) 8.89 (m, 6H), 8.16 (m, 8H), 7.74 (m, 12H). LRMS

(LSIMS) m/z: 705 (M+1).

4.3 Progress towards *meso*-azidomethyl-OEP (85)

meso-formyl-OEP (83)

(83)
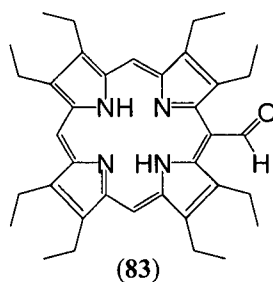
Meso-formyl-OEP was synthesised according to the literature.[32] To a mixture of DMF

(2.00 mL, 21.4 mmol) and POCl₃ (3.52 ml, 44.9 mmol) a solution of copper

octaethylporphyrin (285 mg, 0.47 mmol) in ethylene dichloride (270 mL) was added

dropwise over a period of 20-30 min at 50-60 °C. The mixture was left to stir at this

temperature for 20 min after the addition is complete. The mixture is then cooled to

room temperature and treated with aqueous sodium acetate (250 mL) before stirring for 2

h at 60 °C. The cooled solution is diluted with chloroform (200 mL) which is washed

several times with water, dried and evaporated to dryness. The residue was dissolved in H_2SO_4 (conc.) and kept at 50 °C for 1 h. Ice water (250 ml) with sodium acetate was then poured into the mixture. Enough sodium acetate was added such that the solution was of neutral pH. The mixture is extracted with chloroform, washed with water, dried and evaporated. The product was purified by preparatory TLC (silica, 40 % CH_2Cl_2/hexanes, R_f = 0.45) and obtained in 50 % (130 mg) yield. UV-vis (CH_2Cl_2) λ_{max} (rel. intensity): 405 (1), 505 (0.15), 535 (0.13), 575 (0.13), 625 (0.11). ^{1}H-NMR (300 MHz, $CDCl_3$, ppm) δ 12.75 (s, 1H), 10.0 (s, 2H), 9.9 (s, 1H), 4.05 (m, 12H), 3.85 (q, J = 7.45 Hz, 4H) 1.84 (m, 18H), 1.70 (t, J = 7.45 Hz), -2.95 (s, 2H). LRMS (ESI) m/z: 563 (M+1).

meso-hydroxymethyl-OEP (84)

(84)
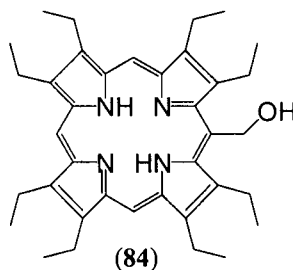
Formyl-OEP was reduced in a similar manner to β-formyl-TTP. A 25 mL round bottom flask was charged with meso-formyl-OEPP (50 mg, 0.09 mmol). The porphyrin was dissolved in THF (25 mL) and stirred for 10 min. $NaBH_4$ (150 mg, 4.3 mmol) was added to the flask, and the mixture was heated at 50°C. The reaction was monitored by TLC and stopped when the starting material was completely consumed (10-15 min). The solvent was evaporated to dryness and the product is extracted from CH_2Cl_2 yielding the dark purple solid (84, 43 mg, 85 %) which was used without further purification. UV-vis

(CH₂Cl₂) λ_{max} (rel. intensity): 405 (1), 505 (0.09), 540 (0.07), 575 (0.05), 630 (0.04). ¹H-NMR (300 MHz, CDCl₃, ppm) δ 10.1 (s, 2H), 9.9 (s, 1H), 6.90 (s, 2H), 4.05 (m, 16H), 1.84 (m, 24H), -2,95 (s, 2H). LRMS (ESI) m/z: 565 (M+1).

4.4   Preparation of β-azido-TPP (86)

β-Nitro-TPP (89)

(89)
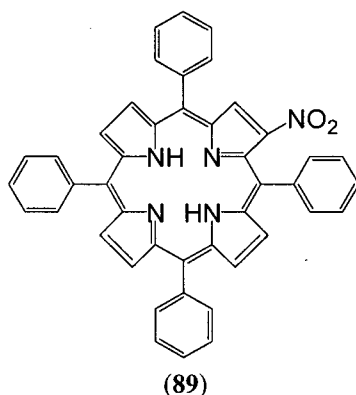
β-Nitro-TPP was synthesised according to Baldwin's method with slight modifications.[123] ZnTPP (400 mg, 0.59 mmol) was dissolved in a mixture of dry CH₂Cl₂ (60 mL) and dry MeCN (20 mL). To the stirred solution was added silver nitrite (130 mg, 0.83 mmol) in MeCN (20 mL) followed by iodine (100 mg, 0.4 mmol) in CH₂Cl₂ (20 mL). When all the ZnTPP was consumed as monitored by TLC, the mixture was filtered through a coarse sintered glass fritted filter. The filtrate was evaporated to dryness and the product was purified by column chromatography (silica, 70 % CH₂Cl₂/hexanes). The product was then demetallated with TFA and worked in the usual way. The purple solid was obtained in 30 % yield (120 mg). R_f = 0.70 (silica, 70 % CH₂Cl₂/hexanes). UV-vis (CH₂Cl₂) λ_{max} (rel. intensity): 427 (1), 526 (0.08), 560 (0.06), 605 (0.03), 605 (0.03). ¹H-

NMR (300 MHz, CDCl$_3$, ppm) δ 9.03 (s, 1H), 8.99 (d, J = 5.06 Hz, 1H), 8.93 (d, J = 4.88

Hz, 1H), 8.87 (m, 2H), 8.69 (bs, 2H), 8.19 (m, 8H), 7.71 (m, 12H), -2.65 (s, 2H). LRMS

(LSIMS) m/z: 660 m/z (M+1).

β-Azido-TPP (86)

(86)
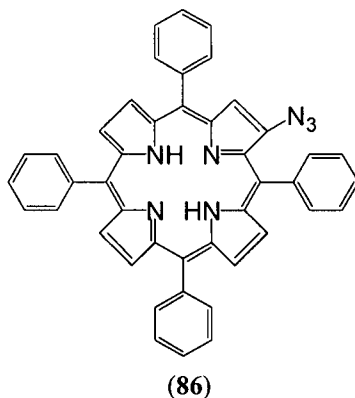
β-Nitro-TPP (150 mg, 0.22 mmol) and 10% palladium (140 mg) on carbon were

suspended in a mixture of MeOH (15 ml) and CH$_2$Cl$_2$. NaBH$_4$ (20 mg, 0.52 mmol) was

added to the mixture. The reaction was monitored by TLC immediately as the starting

material is consumed within 1-2 min. The mixture was filtered (*via* cannule) without

exposure to air through a sintered glass filter. CH$_2$Cl$_2$ was used to wash any residual

porphyrin from the flask and filter and the filtrate evaporated under reduced pressure.

The residue was dissolved in TFA (5 ml) at 0 °C. NaNO$_2$ (80 mg, 1.16mmol) was added

and the mixture stirred for 5 min after which NaN$_3$ (80 mg, 1.23 mmol) was added.

When the mixture ceased to bubble, it was left to stir for 5 min. The mixture was

neutralised with ice water and aqueous saturated sodium acetate and the product extracted

with CH$_2$Cl$_2$. The resulting product (86) is extremely light sensitive, as such

chromatography must be carried out in the dark. The crude product is obtained in high

purity and yield (120 mg, 85% from β-nitro-TPP). R_f = 0.80 (silica, 70% CH_2Cl_2/hexanes). UV-vis (CH_2Cl_2) λ_{max} (rel. intensity): 420 (1), 520 (0.10), 550 (0.03), 595 (0.04), 655 (0.05). I.R. (KBr) : 2103 cm^{-1} (ν_{N_3}). ^{1}H-NMR (300 MHz, CDCl$_3$, ppm) δ 8.87 (d, J = 4.89 Hz, 1H), 8.88 (m, 2H), 8.77 (s, 2H), 8.70 (d, J = 4.89 Hz, 1H), 8.35 (s, 1H), 8.18-8.05 (m, 8H), 7.71 (m, 12H), -2.84 (s, 2H). HRMS (LSIMS) dev. in ppm for mass $C_{44}H_{30}N_7$: -0.19 calculated for 656.25615 m/z (M+1).

β-Azido-CoTPP (92)

A saturated solution of cobaltous acetate in methanol (1 mL) was added to a solution of β-azido-TPP (20 mg) in chloroform (9 mL) and stirred at RT. The reaction was monitored by TLC and until consumption of starting material was complete (~1 hr). The solution was evaporated to dryness and the product was extracted from CH_2Cl_2. The product was obtained in quantitative yield. R_f = 0.75 (silica, 60 % CH_2Cl_2/hexanes). UV-vis (CH_2Cl_2) λ_{max} (rel. intensity): 415 (1), 535 (0.07). I.R. (KBr): 2104 cm^{-1} (ν_{N_3}). LRMS (ESI) m/z = 712 (M+1).

β-Azido-CuTPP (93)

The copper complex was synthesised similarly with copper chloride. The product was obtained in quantitative yield. R_f = 0.70 (silica, 50 % CH_2Cl_2/hexanes). UV-vis (CH_2Cl_2) λ_{max} (rel. intensity): 425 (1), 545 (0.08). I.R. (KBr): 2104 cm^{-1} (ν_{N_3}). LRMS (ESI) m/z = 716 (M+1).

β-Azido-ZnTPP (91)

The zinc complex was synthesised similarly with zinc acetate. The product was obtained in quantitative yield. R_f = 0.50 (silica, 60% CH_2Cl_2/hexanes). UV-vis (CH_2Cl_2) λ_{max} (rel. intensity): 430 (1), 555 (0.06). I.R. (KBr): 2104 cm^{-1} (v_{N_3}). LRMS (ESI) m/z = 718 (M+1).

4.5 Preparation of 5-*para*-azidoperfluorophenyl-10, 15, 20-pentafluorphenylporphyrin (101)

(101)
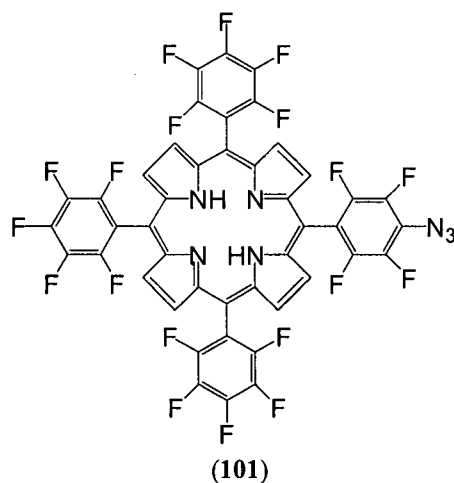
A mixture of NaN_3 (33.4 mg, 0.51 mmol), pFTPP (50.0 mg, 0.051 mmol), acetone (4 mL) and water (0.5 mL) was refluxed for 8 h. The mixture was evaporated under reduced pressure (removing only the acetone), washed with water and extracted from CH_2Cl_2. The product was isolated by preparatory TLC (silica, 40% CH_2Cl_2/hexanes, R_f = 0.75) and obtained in 15% yield (7.5 mg). UV-vis (CH_2Cl_2) λ_{max} rel. intensity): 415 (1), 505 (0.07), 585 (0.03). I.R. (KBr) : 2127 cm^{-1} (v_{N_3}). ^{1}H-NMR (300 MHz, $CDCl_3$, ppm) δ 8.90 (s, 8H), -2.95 (s, 2H). ^{19}F-NMR (282 MHz, $CDCl_3$, ppm) δ -136.9 (dd, J_p = 8.46 Hz, J_o = 22.56 Hz, 6F) –137.6 (dd, J_p = 8.46Hz, J_o = 22.56 Hz, 2F), -151.7 (t, J_o = 19.74

Hz, 3F), -152.0 (dd, J_p = 11.28 Hz, J_o = 22.56 Hz, 2F), -161.8 (dt, J_p = 8.46 Hz, J_o = 22.56 Hz, 6F). HRMS (LSIMS) dev. in ppm for mass $C_{44}H_{11}N_7F_{19}$: 3.89 calculated for 998.08114 m/z (M+1).

Thermolysis of (101)

10 mg (0.01 mmol) of **101** was dissolved in toluene and refluxed under N_2 for 42 h. The product was purified by preparatory TLC (R_f = 0.5, silica, 40% CH_2Cl_2/hexanes), obtained in 10% yield (1 mg) and identified as **103**.
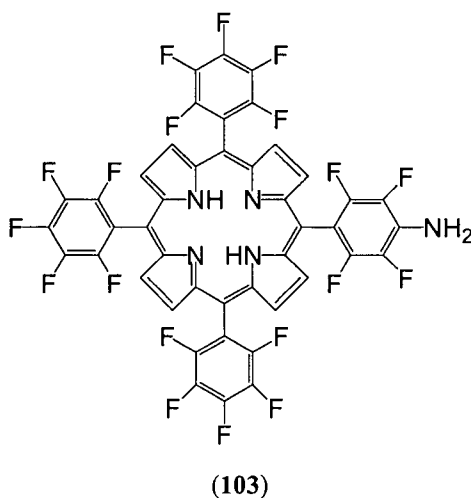
(103)

UV-vis (CH_2Cl_2) λ_{max} rel. intensity): 415 (1), 505 (0.07), 585 (0.03). ^{1}H-NMR (300 MHz, CDCl₃, ppm) δ 8.90 (s, 2H), 8.80 (s, 6H), 4.48 (s, 2H), -2.95 (s, 2H). ^{19}F-NMR (282 MHz, CDCl₃, ppm) δ -136.9 (dd, J_p = 8.46 Hz, J_o = 22.56 Hz, 6F) –140.9 (dd, J_p = 8.46Hz, J_o = 22.56 Hz, 2F), -152.0 (m, 3F), -161.9 (m, 6F), -162.4 (dd, J_p = 8.46 Hz, J_o = 22.56 Hz, 6F). HRMS (LSIMS) dev. in ppm for mass $C_{44}H_{13}N_5F_{19}$: -0.14 calculated for 972.08662 m/z (M+1).
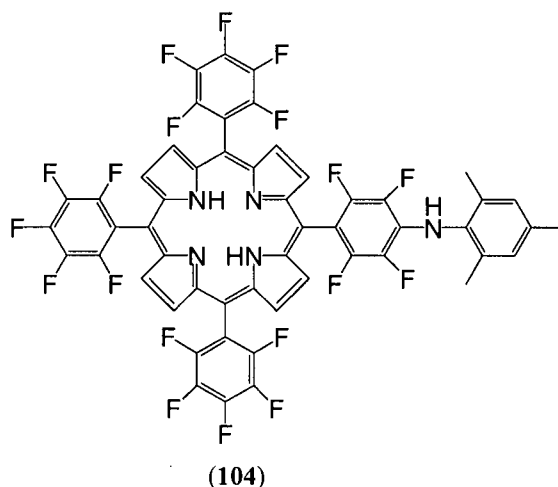
Compound **101** was similarly thermolysed in mesitylene to yield **104** as a purple solid in 40 % yield.

(104)

R_f = 0.80 (silica, 40% CH_2Cl_2/hexanes). UV-vis (CH_2Cl_2) λ_{max} rel. intensity): 415 (1), 505 (0.07), 585 (0.03). ^{1}H-NMR (300 MHz, $CDCl_3$, ppm) δ 9.00 (s, 2H), 8.80 (s, 6H), 7.0 (s, 2H), 5.69 (s, 1H), 2.44 (s, 6H), 2.30 (s, 3H), -2.95 (s, 2H). HRMS (ESI) dev. in ppm for mass $C_{53}H_{23}N_5F_{19}$: -0.3 calculated for 1090.1650 m/z (M+1).

Photolysis of (101)

10 mg of **101** was placed in a Pyrex tube, dissolved in toluene (10mL) and degassed. The mixture was then photolysed at 350 nm for 12 h. The mixture was worked up as before and **103** was obtained in 10 % yield (1 mg).

Compound **101** was photolysed similarly in mesitylene yielding **104** in 10 % yield.

5 References

1   Milgrom, L.R. *The Colours of Life;* Oxford University Press: New York, **1997**, pp 1-90.

2   Campbell, N. A. *Biology*, 3rd ed.; Benjamin/Cummins: New York, **1993**, pp 199–217.

3   Fischer, H.;Orth, H. *Die Chimie des Pyrrols,* Acadamische Verlagsgesellschaft: Leipsig, **1934-1940**, Vol I-III.

4   Lindsey, J. S. In *The Porphyrin Handbook*; Kadish, K. M.; Smith, K. M.; Guilard, R. Ed; Academic Press; New York, **1998**, Vol 1, pp 46-47.

5   Smith, K. M. In *The Porphyrin Handbook*; Kadish, K.M.; Smith, K. M.; Guilard, R. Ed; Academic Press; New York, **1998**, Vol 1, pp 2-41.

6   Sessler, J. L.; Mozaffari, A.; Johnson, M. R. *Org. Synth.* **1991**, *70*, 68.

7   Ono, N.; Kawamura, H.; Bougauchi, M.; Maramura, K. *Tetrahedron* **1990**, *46*, 7483.

8   Fischer, H.; Klarer, J. *Ann. Chem.* **1926**, *448*, 178.

9   MacDonald, S. F.; Bullock, E.; Arsenault, G. P. *J. Am. Chem. Soc.* **1960**, *82*, 4384.

10   Rothemond, P. *J. Am. Chem. Soc.* **1935**, *57*, 2010.

11   Rothemond, P.; Menotti, A. R. *J. Am. Chem. Soc.* **1941**, *63*, 267.

12   Alder, A. D.; Longo, F. R.; Finarelli, J. D.; Goldmacher, J.; Assour, J.;Korsakoff, L. *J. Org. Chem.* **1967**, *32*, 476.

13   Lindsey, J. S.; Scriemann, I. C.; Hsu, H. C.; Kearney, P. C.; Marguerettaz, A. M. *J. Org. Chem.* **1987**, *52*, 827.

14   Kuster, W, Z. *Physiol. Chem.* **1912**, *82*, 463.

15   Fischer, H.; Zeile, K. *Ann. Chem.* **1929**, *486*, 98.

16   Ollis, W. D. In *Aromaticity, an International Symposium*; The Chemical Society; Burlington House; **1966**, *21*, 3.

17   Vincente. In *The Porphyrin Handbook*; Kadish, K.M.; Smith, K. M.; Guilard, R. Ed; Academic Press; New York, **1998**, Vol 1, pp 150-195.

18   Janson, T.; Katz, J. In *The Porphyrins*; Dolphin, D. Ed; Academic Press; New York, **1978**, Vol IV, pp 1-54.

19   Smith, K,M. In *Porphyrins and Metalloporphyrins*, Smith, K, M. Ed.; Elsevier; Amsterdam, **1975**, pp 399.

20   Buchler, J. In *The Porphyrins*; Dolphin, D. Ed; Academic Press; New York, **1978**, Vol I, pp 300-474.

21   Woodward, R. B. *Ind. Chim. Belge* **1962**, *11*, 1293.

22   Fuhrhop, J.-H.; Subramanian, J. *Phil. Trans. R. Soc. Lond. B.* **1976**, *273*, 335. Spangler, D.; Maggiora, G. M..; Shipman, L. L.; Christofferson, R. E. *J. Am. Chem. Soc.* **1977**, *99*, 7470.

23   Samuels, E.; Shuttleworth, R. Stevens, T. S. *J. Chem. Soc. (C).* **1968**, 145.

24   Jaquinod, L. In *The Porphyrin Handbook*; Kadish, K.M.; Smith, K. M.; Guilard, R. Ed. Academic Press; New York, **1998**, Vol 1, pp 200-237.

25   Grigg, R.; Shelton, G.; Sweeny, A.; Johnson, A. W. *J. Chem. Soc., Perkin Trans. 1* **1972**, 1789.

26   Bonnett, R.; Ridge, R. J.; Appelman, E. H. *J. Chem. Soc., Chem. Commun.* **1978**, 310.

27   Shea, K. M.; Jaquinod, L.; Denat, F.; Smith, K. M. *J. Chem. Soc., Chem. Commun.* **1998**, 759.

28   Momenteau, M.; Look, B.; Bisagni, E. *Can. J. Chem.* **1979**, 1804.

29   Callot, H. J.; Schaeffer, E.; Cromer, R.; Metz, F. *Tetrahedron* **1990**, *46*, 5253.

30   Buchler, J. W.; Dreher, C.; Herget, G. *Liebigs Ann. Chem.* **1988**, 43.

31   Ponomarev, G. V.; Marvin, G. B. *Chemistry of Heterocyclic Compounds.* **1982**, *18*, 50.

32   Fuhrhop, J. -H.; Smith, K,M. In *Porphyrins and Metalloporphyrins*, Smith, K, M. Ed.; Elsevier; Amsterdam, **1975**, pp 818.

33   Buchler, J. W.; Dreher, C.; Herget, G. *Liebigs Ann. Chem.* **1988**, 43.

34   Callot, H. J. *Bull. Soc. Chim. Fr.* **1973**, 3413.

35   Callot, H. J. *Tetrahedron* **1973**, *29*, 899.

36 Bonfantini, E. E.; Officer, D. L. *Tetrahedron Lett.* **1993**, *34*, 8531.

37 Bonnett, R.; Stephenson, G. F. *J. Org. Chem.* **1965**, *30*, 2791.

38 Johnson, A. W.; Winter, M. *Chem. Ind. (London).* **1975**, 351

39 Baldwin, J. E.; Crossley, M. J.; DeBernardis, J. *Tetrahedron.* **1992**, *38*, 685.

40 Barnett, G. H.; Smith, K. M. *J. Chem. Soc., Chem. Commun.* **1975**, 772.

41 Barnett, G. H.; Smith, K. M., Evans, B.; Martynenko, Z. *J. Am. Chem. Soc.* **1979**, *101*, 5953.

42 Johnson, C.; Dolphin, D. *Tetrahedron Lett.* **1976**, 2197.

43 Cavaleiro, J. A. S.; Hombrecher, H. K.; Gherdan, V. M.; Ohm, S.; *Tetrahedron* **1993**, *49*, 8569.

44 Crossley, M. J.; Harding, M. M.; Tansey, C. W. *J. Org. Chem.* **1994**, *59*, 4433.

45 Crossley, M. J.; King, L. G.; *J. Chem. Soc., Perkin Trans. 1.* **1996**, 1251.

46 Shea, K. M.; Jaquinod, L.; Denat, F.; Smith, K. M. *J. Chem. Soc., Chem. Commun.* **1998**, 759.

47 Frydman,B.; Frydman, R.; Valasinas, A.; Bogorad, L. In *The Porphyrins*; Dolphin, D. Ed; Academic Press; New York, **1978**, Vol VI, Chapter 1 – 2.

48 Gouterman, M. In *The Porphyrins*; Dolphin, D. Ed; Academic Press; New York, **1978**, Vol III, Ch. 1.

49 Gouterman, M. *J. Chem. Phys. Chem.* **1959**, *30*, 1139.

50 Fajer, J. *Chem. Ind.* **1991**, 861.

51 March, J. *Advanced Organic Chemistry,* 4th dd.; Wiley-Interscience: New York, **1992**, pp 241.

52 Sternberg, E. D.; Dolphin, D. *Tetrahedron* **1998**, *54*, 4151.

53 Henderson, B. W.; Dougherty, T. J., Eds.; *Photodynamic Therapy: Basic Principles and Clinical Application;* Marcel Dekker: New York, **1992**.

54 Meyer-Betz, F. *Arch. Dtsch. Klin. Med.* **1913**, *112*, 476.

55   Auler, H.; Banzer, G. Z. *Krebsforsch.* **1942**, *53*, 65.

56   Figge, F. H. J.; Weiland, G. S.; Mangianiello, L. O. *J. Roy. Soc. Exp. Bio. Med.* **1948**, *68*, 640.

57   Schwartz, S.; Absolon, K.; Vermund, H. *Univ. Minnesota Med. Bull.* **1955**, *7*, 7.

58   Lipson, R. L.; Blades, E. J.; Olsen, A. M. *J. Natl. Cancer Inst.* **1961**, *26*, 1.

59   Lipson, R. L.; Gray, M. J.; Blades, E. J. *Proc. 9th Intl. Cancer Congress* **1966**, Tokyo, Japan.

60   Dougherty, T. L.; Kaufman, J. H.; Goldfarb, A.; Weishaupt, K. R.; Boyle, D.; Mittleman, A. *Cancer Res.* **1978**, *38*, 2628.

61   http://www.qlt-pdt.com

62   Dolphin, D. *Can. J. Chem.* **1994**, *72*, 1005.

63   Ricchelli, F. *J. Photochem. Photobiol., B* **1995**, *29*, 109.

64   Moan, J. *J. Photochem. Photobiol., B* **1990**, *6*, 343.

65   Ochsner, M. *J. Photochem. Photobiol., B* **1997**, *39*, 1.

66   Moore, J.; West, C. M. L.; Whitehurst, C. *Phy. Med. Biol.* **1997**, *42*, 913.

67   Hendrson, B. W.; Waldow, S. M.; Mang, T. S.; Potter, W. R.; Malone, P. B.; Dougherty, T. J. *Cancer Res.* **1986**, *46*, 2532.

68   Luna, M. C. l.; Gomer, C. J. *Cancer Res.* **1991**, *51*, 4243.

69   Sharkey, S. H.; Wilson, B. C.; Moorehead, R.; Singh, G. *Cancer Res.* **1993**, *53*, 4994.

70   Pandey, R. K.; Zheng, X. In *The Porphyrin Handbook*; Kadish, K.M.; Smith, K. M.; Guilard, R. Ed; Academic Press; New York, **1998**, Vol 6, pp 185-225.

71   Davis, S.; Weiss, M. J.; Wong, J. R.; Lampidis, T. J. *J. Biol. Chem.* **1985**, *260*, 13844.

72   Bonnett, R. *Chem. Soc. Rev.* **1995**, 19.

73   Gust, D.; Moore, T. A.; Moore, A. M., Seely, G. R.; Stone, S.; Lin, S.; Hung, S. –C.; Liddell, P. A.; Kuciauskas, D. *J. Phys. Chem. B.* **1997**, *101*, 429.

74 Griffiths, M.; Sistrom, W. R.; Cohen-Bazire, G.; Stanier, R. Y. *Nature* **1955**, *176*, 1211.

75 Snyder, R.; Arvidson, E.; Foote, C.; Harrigan, L.; Christensen, R. L. *J. Am. Chem. Soc.* **1985**, *105*, 4117.

76 Deming-Adams, B. *Biochim. Biophys. Acta* **1990**, *1020*, 1.

77 Gust, D.; Moore, T. A. In *The Porphyrin Handbook*; Kadish, K. M.; Smith, K. M.; Guilard, R. Ed; Academic Press; New York, **1998**, Vol 8, pp 154-159.

78 Kong, J.; Loach, P. A. In *Frontiers of Biological Energetics: From Electrons to Tissues*. Dutton, P. L.; Leigh, J. S.; Scarpa, H. Ed; Academic Press, New York, **1978**, p.73.

79 Tabushi, I.; Koga, N.;Yanagita, M. *Tetrahedron Lett.* **1979**, 257.

80 Gust, D.; Moore, T. A. *Top. Curr. Chem.* **1991**, *159*, 103.

81 Bouchet, M. J.; Goeldner, M. *Photochem. Photobiol.* **1997**, *65*, 195.

82 Bayley, H.; Staros, J. V. In *Azides and Nitrenes*; Scriven, E. S. V. Ed; Academic Press: Orlando, **1984**, pp 434-487.

83 Westheimer, F. H.; Singh, A.; Thorton, E. R. *J. Biol. Chem.* **1962**, *237*, PC 3006.

84 Knowles, J. R.; Fleet, G. W. J.; Porter, R. R. *Nature (London)*. **1969**, *224*, 511.

85 Knowles, J. R. *Acc. Chem. Res.* **1972**, *5*, 155. Chowdhry, V; Westheimer, F.H. *Annu. Rev. Biochem.* **1977**, *46*, 69.

86 Fleming, S. A. *Tetrahedron* **1995**, *51*, 12479.

87 Bayley, H.; Knowles, J. R. *Biochemistry*. **1978**, *17*, 2414. Brunner, J.; Richards, F. M. *J. Biol. Chem.* **1980**, *255*, 3319.

88 Smith, P. A. In *Azides and Nitrenes*; Scriven, E. S. V. Ed; Academic Press: Orlando, **1984**, pp 35-107.

89 Platz, M. S.; Leyva, E.; Munoz, D. *J. Org. Chem.* **1989**, *54*, 5938.

90 Reiser, A.; Leyshon, L. J. *J. Am. Chem. Soc.* **1970**, *92*, 7487.

91 McRobbie, I. M.; Meth-Conn, O.; Suschitzky, H. *Tetrahedron Lett.* **1976**, 425.

92   Smith, P. A. S.; Boyer, J. H. *Org. Synth. Coll.* **1963**, *IV*, 75.

93   Grieco, P. A.; Mason, J. P. *J. Chem. Eng. Data* **1967**, *12*, 623.

94   de Montellano, P. R. O.; Medzihradszky, K. F.; Tschirret-Guth, R. A. *J. Chem. Soc.* **1998**, *120*, 7404.

95   Leyve, E.; Platz, M. S.; Persy, G.; Wirz, J. *J. Am. Chem. Soc.* **1986**, *108*, 3783.

96   Meijer, E. W.; Nijhuis, S.; Van Vroonhoven, F. C. B. M. . *J. Am. Chem. Soc.* **1988**, *110*, 8092

97   Brown, R. L.; Gerber, W. V.; Karpen, J. W. *Proc. Natl. Acad. Sci. U.S.A.* **1993**, *90*, 5369.

98   Resek, J. F.; Ruoho, A. E. *J. Biol. Chem.* **1988**, *263*, 14410.

99   Yang, C. P. H.; Mellado, W. Horwitz, S. B. *Biochem. Pharmacol.* **1988**, *13*, 1417.

100 Escher, E. *Pharmacol. Ther.* **1988**, *37*, 37.

101 Ruat, M.; Koerner, M.; Garbarg, M.; Gros, C.; Schwartz, J. C.; Tertiuk, W.; Ganellin, R. *Proc. Natl. Acad. Sci. U.S.A.* **1988**, *85*, 2743.

102 Banks, R. E.; Sparkes, G. R. *J. Chem. Soc., Perkin Trans. 1* **1972**, 2964

103 Dunkin, I. R.; Thomson, P. C. P. *J. Chem. Soc., Chem. Commun.* **1982**, 1192.

104 Leyva, E.; Platz, M. S.; Persy, G.; Wirz, J. *J. Am. Chem. Soc.* **1986**, *108*, 8307.

105 Young, M. J. T.; Platz, M. S. *Tetrahedron Lett.* **1989**, *30*, 2199.

106 Keana, J. W. F.; Cai, S. X. *J. Org. Chem.* **1990**, *55*, 3640.

107 March, J. *Advanced Organic Chemistry*, 3rd ed; Wiley-Interscience: New York, **1985**, pp 166.

108 March, J. *Advanced Organic Chemistry,* 4th ed; Wiley-Interscience: New York, **1992**, pp 20.

109 Birchall, J. M.; Haszeldine, R. N.; Jones, M. E. *J. Chem. Soc. C.* **1971**, 1344.

110 Battioni, P.; Brigaud, O.; Desvaux, H.; Mansuy, D. Traylor, T. G. *Tetrahedron Lett.* **1991**, *32*, 2893.

111 Smith, R. A. G.; Knowles, J. R. *J. Am. Chem. Soc.* **1973**, *95*, 5072.

112 Brunner, J.; Senn, H.; Richards, F. M. *J. Biol. Chem.* **1980**, *255*, 3313.

113 Ojima, I.; Nakanishi, K.; Lin, S.; Fang, K.; Hashimoto, M. *Tetrahedron Lett.* **2000**, *41*, 4287.

114 Guenard, D.; Gueritte-Vogelein, F.; Potier, P. *Acc. Chem. Res.* **1993**, *26*, 160.

115 Carr, S. A.; Huddleston, M. J.; Annan, R. S. *Annal. Biochem.* **1996**, *239*, 180.

116 Desjardins, A. M. M. Sc. Thesis, The University of British Columbia, Vancouver, British Columbia, **2000**.

117 Van Auken, R. *J. Am. Chem. Soc.* **1962**, *84*, 3736.

118 March, J. *Advanced Organic Chemistry*, 4th ed; Wiley-Interscience: New York, **1992**, pp 396.

119 Viaud, M. C.; Rollin, P. *Synthesis* **1990**. 131.

120 Abramovitch, R. A.; Kyba, E. P. In *The Chemistry of the Azido Group*; Patai, S. Ed. Wiley, New York, **1970**. Ch.5.

121 March, J. *Advanced Organic Chemistry*, 4th ed; Wiley-Interscience: New York, **1992**, pp 884.

122 Lewis, F. D.; Saunders, Jr. W. H. *J. Am. Chem. Soc.* **1968**, *90*, 7033.

123 Baldwin, J. E.; Crossley, M. J.; DeBernardis, J. *Tetrahedron* **1992**, *38*, 685.

124 Smith, P. A. S.; Brown, B. B. *J. Am. Chem. Soc.* **1951**, *73*, 2438. Hegarty. In *The Chemistry of the Azido Group*; Patai, S. Ed. Wiley, New York, **1978**. pp 511-591.

125 Kanakarajan, K.; Haider, K.; Czarnik, A. W. *Synthesis* **1988**, 566.

126 Shuster, G. B.; Shrock, A. K. *J. Am. Chem. Soc.* **1984**, *106*, 5228.

127 Abramovitch, R. A.; Challand, S. R.; Scriven, E. F. V. *J. Am. Chem. Soc.* **1972**, *94*, 1374.

128 D. Dolphin, personal communication.

129 Bonnett, R.; Stephenson, G. F. *J. Org. Chem.* **1965**, *30*, 2791.

130 Billig, M. J.; Baker, E. W. *Chem. Ind. (London)* **1969**, 654.

131 Arnold, D. P.; Bott, R. C.; Eldridge, H.; Elms, F. M.; Smith, G.; Zojaji, M. *Aust. J. Chem.* **1997**, *59*, 495.

132 Bovey, F. A. In *Nuclear Magnetic Resonance Spectroscopy.;* New York: Academic Press, **1969**, pp 444.

133 Treinin, A. In *The Chemistry of the Azido Group*; Patai, S. Ed; Interscience; New York, **1971**, pp 3.

134 Spagnolo, P.; Zanirato, P. *Tetrahedron Lett.* **1987**, *28*, 961.

135 Hatanaka, Y.; Nakayama, H.; Kanaoka, Y. *Heterocycles.* **1993**, *35*, 997.